Department of Biomedical Sciences
University of Veterinary Medicine Vienna

Institute of Pharmacology and Toxicology

(Head: O.Univ.-Prof. Dr.med.vet. Mathias Müller)

Circular peptide therapeutics for Acute Myeloid Leukemia

Master Thesis

University of Veterinary Medicine Vienna

Submitted by
Zuzanna Edyta Kieron

Vienna, July 2023

Supervision

Karoline Kollmann, PhD
Department for Biomedical Sciences
Institute of Pharmacology and Toxicology
University of Veterinary Medicine Vienna

Reviewer

Univ.-Prof. Dr. Dagmar Stoiber-Sakaguchi,
Department Pharmacology, Physiology and Microbiology
Division Pharmacology
Karl Landsteiner University of Health Sciences Krems an der Donau

Abstract

Acute myeloid leukemia (AML) is characterized by an aggressive clinical course and a high mortality rate. It is driven by leukemic stem cells with a highly heterogeneous mutational background, resulting in different subtypes. The properties of leukemic stem cells (e.g., epigenetic pattern, signaling) differ from those of the mass AML population, making these cells difficult to eliminate. The standard of care for patients has changed only minimally over the past four decades, and there is an urgent need to develop patient-specific treatment options.

Previous studies and preliminary data suggest that plant-derived circular peptides may be novel treatment options for AML. We use a mouse model of hematopoietic progenitor cells (HPCLSK) to mimic AML subtypes. These cells can repopulate the entire hematopoietic cell pool and induce disease in vivo after transformation. In the study two different AML oncogenes (RUNX1-RUNX1T1 and KMT2A-MLLT3) were used to elute the efficacy of the natural cyclotide Caripe 11 and 8 as well as the synthetic prototype cyclotide T20K for AML. The effects on cell viability were analyzed using flow cytometry based viability assays. The underlying mechanisms of the tested cyclotides were investigated by analyses of proliferation, apoptosis, and myeloid differentiation. The level of apoptosis-related proteins was determined after T20K treatment by using Western Blots.

We determined the IC50 values of Caripe (1.3 - 2.4µM) and T20K (5-10 µM) for biological replicates of RUNX1-RUNX1T1+ and KMT2A-MLLT3+ cell lines. The results of cell viability assays revealed that the cyclotides lowered the cell viability of distinct biological replicates to a different degree. Caripe treatment of murine AML cells induced apoptosis and T20K treatment induced apoptosis and necrosis. Moreover, Caripe treatment did not induce myeloid differentiation. T20K treatment altered the levels of apoptosis-related proteins. RUNX1-RUNX1T1+ cells increased levels of Bcl-xl and p53 and lowered levels of ATM upon T20K treatment.

The tested cyclotides show a promising natural product-based treatment option for AML subtypes. Our preliminary results open a novel research area investigating in depth the mechanisms underlying cyclotide treatment and possible novel combinatorial treatment strategies.

List of Abbreviations

7AAD	7-aminoactinomycin D
ALCL	Anaplastic large cell lymphoma
ALL	Acute lymphoblastic leukemia
AML	Acute myeloid leukemia
AML1	Acute myeloid leukemia 1 protein
APS	Ammonium persulfate
ATM	Ataxia telangiectasia mutated kinase
ATP	Adenosine triphosphate
BCA	Bicinchoninic acid
BCL6	B-cell lymphoma 6
BSA	Bovine serum albumin
CCK2R	Cholecystokinin-2 receptor
CCNM	Cyclic cysteine knot motif
CDK8	Cyclin-dependent kinase 8
CLPs	Common lymphoid progenitors
CMPs	Common myeloid progenitors
CRF1R	Corticotropin-releasing factor type 1 receptor
CTG	CellTiter-Glo Reagent®
DMSO	Dimethyl sulfoxide
DNMT3A	DNA nucleotide methyltransferase 3A
EAE	Experimental autoimmune encephalomyelitis
FAB	French American British
FACS	Fluorescence-activated cell sorting
FCS	Fetal calf serum

FLT3	FMS-like tyrosine kinase 3
FMO	Fluorescence minus one
GMPs	Granulocyte-macrophage progenitors
GPCR	G protein-coupled receptor
GPI	Glycosylphosphatidylinositol
HEK	Human embryonic kidney
hIL-6	Human interleukin-6
HPC^{LSK}	Hematopoietic progenitor cells
HRP	Horseradish peroxidase
HSCs	Hematopoietic stem cells
IC	Intensive chemotherapy
IC_{50}	Inhibitory concentration
IDH1	Isocitrate dehydrogenase 1
IL-2	Interleukin 2
IMDM	Iscove's Modified Dulbecco's Medium
ITD	Internal tandem duplication
JAK2	Janus kinase 2
LMPPs	Lymphoid primed multipotent progenitors
LSCs	Leukemic stem cells
MAPK	Mitogen-activated protein kinase
MEP	Megakaryocyte erythroid progenitors
MFI	Mean Fluorescence Intensity
MLL	Mixed lineage leukemia
MPPs	Multipotent progenitors
MS	Multiple sclerosis
mTOR	Mammalian target of rapamycin

PBS	Phosphate-buffered saline
PI	Propidium iodide
PVDF	Polyvinylidene difluoride
RP-HPLC	Reversed-phase high-performance liquid chromatography
RT	Room temperature
RUNX1	Runt-related transcription factor 1
SCF	Stem cell factor
SCT	Stem cell transplantation
SDS	Sodium dodecyl (lauryl) sulfate
SDS-PAGE	Sodium dodecyl sulphate polyacrylamide gel electrophoresis
SEM	Standard deviation error of the mean
STAT5	Signal transducer and activator of transcription 5
T20K	The synthetic version of kalata B1 cyclotide
TEMED	N,N,N′,N′-Tetramethyl ethylenediamine
TET2	Ten-eleven translocation 2
TKD	Tyrosine kinase domain
TP53	Tumor protein p53

TABLE OF CONTENTS

1 INTRODUCTION

1.1 ACUTE MYELOID LEUKEMIA

Hematopoiesis refers to the commitment and differentiation processes that lead to the formation of all blood cells from hematopoietic stem cells (HSCs). The process of hematopoiesis typically involves the activation of HSCs that are capable of self-renewal, leading to the formation of multipotent progenitors (MPPs). These MPPs can differentiate into several types of progenitors, such as lymphoid primed multipotent progenitors (LMPPs), common myeloid progenitors (CMPs), common lymphoid progenitors (CLPs), granulocyte-macrophage progenitors (GMPs), and megakaryocyte erythroid progenitors (MEP)[1–3]. CLPs are responsible for generating T-cells, B-cells, and NK-cells, while CMPs produce a variety of cell types including macrophages, erythrocytes, platelets, and granulocytes[4,5]. However, mutations in HSCs and progenitor cells can result in pre-leukemic stem cells, which can eventually transform into leukemic stem cells (LSCs) (Figure 1). In some cases, this transformation occurs without a clinically recognized pre-leukemic phase, but typically more than one mutation is required to generate acute leukemia. LSCs can arise from a limited progenitor through secondary mutations that confer self-renewal. The development of Acute Myeloid Leukemia (AML) begins with the transformation of normal HSCs, MPPs, or more committed progenitors into LSCs, which can ultimately lead to the development of leukemia[6].

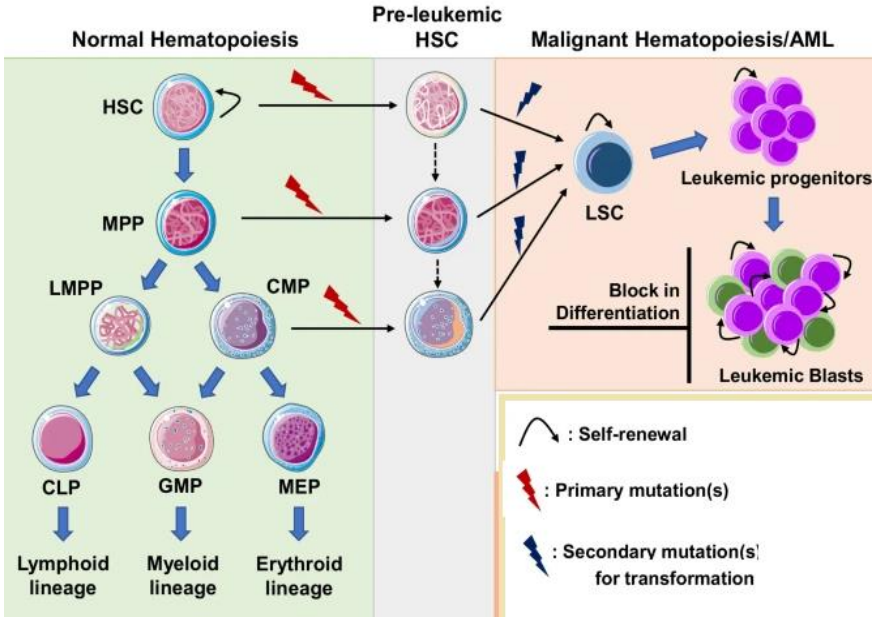

Figure 1: Normal and malignant hematopoiesis (adapted from Long et al., 2022)

AML is a heterogeneous neoplasm in which various subtypes can be distinguished. These subtypes refer to several myeloid differentiation steps: myeloblasts, promyelocytes, monoblasts, promonocytes, erythroblasts, and megakaryoblasts. In the case of AML, the leukemic stem cells accumulate in the bone marrow and translocate to the peripheral blood and replace the normal blood cell populations, giving rise to the disease. In turn, this leads to severe cytopenia, immune failure, and also dysregulation of coagulation pathways[7]. The etiology of the disease remains not very clear[8]. However, it is known that environmental factors and family background are playing a key role in the development of AML. Environmental influences listed as the most prominent are ionizing radiation, therapeutic agents, and occupational exposure to chemicals[8]. The development of leukemia involves multiple steps and depends on the ability of a type of blood cell to respond to certain triggers at different stages. The various subtypes of AML may have different underlying causes, possibly related to specific genetic mutations or abnormalities[9]. While some cases of AML may be linked to known environmental factors, many cases appear to arise spontaneously without any obvious cause[10].

AML is a rare type of cancer. It is estimated that approximately 0.5 percent of men and women will be diagnosed with AML at some point during their lifetime[11]. It is the most common acute leukemia in adults and the second most common in children[12]. Besides its cell type heterogeneity, AML also has genetic heterogeneity and is genetically pleiomorphic[13]. AML is classified into different subtypes. The classification of AML is based on the appearance of cell types and their genetic abnormalities. This is in contrast to most cancers and tumors, which are classified based on the type of cell, how aggressive they are, and whether they spread to other organs[2]. There are two major classification systems used to categorize AML subtypes, the French American British (FAB) classification, which has been replaced by the newer World Health Organization (WHO) classification. The FAB classification system for leukemia fails to consider certain factors that may impact the prognosis of AML, like specific cytogenetic findings and AML associated with myelodysplasia[16]. As a result, the WHO has proposed a newer system that accounts for some of these factors to classify AML. This system groups AML into several categories, including AML with genetic abnormalities, AML with mutated TP53 (a common tumor suppressor), AML with multilineage dysplasia, AML related to prior chemotherapy or radiation, and unspecified AML (Figure 2). Occasionally, ALL with myeloid markers may be classified as AML with lymphoid markers, mixed lineage leukemias, or undifferentiated or biphenotypic acute leukemias (due to both lymphocytic and myeloid features)[2].

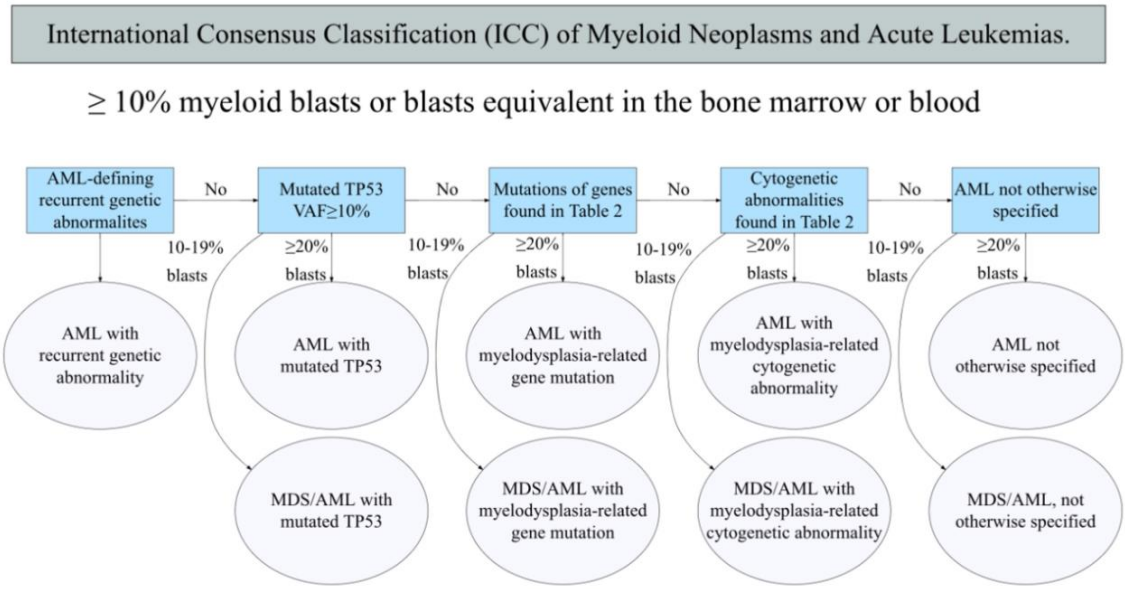

Figure 2: Classification scheme of AML using the International Consensus Classification (Adapted from Hang and Kuzu, 2022)[17].

The median age of presentation of this neoplasm is 69 years [11]. It is a very aggressive disease, and the prognosis for patients is poor [18]. Little progress was achieved in the last few decades regarding older patients, where aggressive therapies cannot be applied. Patients over age 65 are not legitimate for intensive chemotherapy (IC) and allogeneic stem cell transplantation (allo-SCT)[19]. The combination of anthracycline and cytarabine for induction therapy, the "3 + 7" regimen which entails 7 days of continuous infusion of cytarabine in combination with 3 consecutive days of anthracycline treatment (typically daunorubicin) remains the standard therapy for almost five decades. The long-term disease-free survival of AML patients did not change for patients under age 60[18]. Therefore, a new therapeutic approach for AML patients is of great need.

1.2 FUSION ONCOGENES IN AML

Three major AML subtypes exist according to their genetic aberrations, AML with kinase mutations (e.g. FLT3 (30%), c-KIT (5%) and JAK2 (2%)[20]), translocations (e.g. t (15; 17), t (8; 21), inv and 11q23/MLL with frequencies between 3 and 10%[21]) or mutations in epigenetic modifiers (e.g. *DNMT3A* (DNA nucleotide methyltransferase 3A) (18-22%), *TET2* (ten-eleven translocation 2) (7-25%), and *IDH1/2* (isocitrate dehydrogenase 1/2) (10-14%) [22])). FMS-like tyrosine kinase 3 (FLT3) is a type III receptor tyrosine kinase and plays a crucial role in the survival, proliferation, and differentiation of hematopoietic cells. Mutation of the *FLT3* gene is a very common genetic alteration in AML patients and is associated with a poor prognosis[23]. *FLT3* mutations can be categorized into two types: internal tandem duplication mutations in the juxtamembrane domain (*FLT3*-ITD) and point mutations or deletions in the tyrosine kinase domain (*FLT3*-TKD). Both types of mutations activate the FLT3 receptor without needing a ligand, triggering several intracellular signaling pathways, including STAT5, MAPK, and AKT signals. This ultimately leads to cell proliferation and anti-apoptosis[23,24].

It has been noticed that the translocation between chromosomes 8 and 21 (t(8;21)) in AML patients is relatively common since it accounts for occurring in approximately 4%–12% of adults and 12%–30% of pediatric patients[25]. In this translocation, runt-related transcription factor 1(*RUNX1*), acute myeloid leukemia 1 protein (*AML1)* gene, on the long arm of chromosome 21 (q22), fuses with the *RUNX1T1* (acute myelogenous leukemia 1 translocation 1) gene on the long arm of chromosome 8 (q22), leading to s a RUNX1/RUNX1T1 chimeric product[8]. The N-terminal part of RUNX1 is essential for the transcription of various genes related to myeloid and lymphoid differentiation. The C-terminal component of RUNX1T1 is important for transcriptional co-regulation of (write which genes as for the N-terminal part). The RUNX1/RUNX1T1 fusion product reduces apoptosis of the transformed cells by activating the expression of the anti-apoptotic gene BCL-2[8].

One example of a fusion oncogene of an epigenetic regulator in AML is the translocation of chromosomes 9 and 11 t(9;11). *KMT2A* is located at chromosome 11q23, encoding the histone lysine-specific N-methyltransferase 2A. The *KMT2A* gene encodes a lysine methyltransferase (KMT), which is crucial for the process of hematopoiesis. It acts as a transcriptional co-activator and plays a vital role in regulating gene expression during the early stages of development.

Additionally, it also controls the expression of circadian genes, which is essential for maintaining the body's internal clock[26]. Over 90 *KMT2A* fusion partners have been identified so far. The most recurring ones are *AFF1*, *MLLT1*, and *MLLT3*. They all encode proteins regulating epigenetic mechanisms[27].

1.3 CYCLOTIDES

Currently used drugs can be divided into two groups. The so-called "small molecules" are <500 Da and the “biologics” consist of large molecules, <5000 Da[28]. The small molecules are applied orally but sometimes show reduced selectivity and therefore often encounter side effects. "Biologics" have many more interactions with the targets specific to them and in this case the selectivity is not reduced. On the downside, biologics have overall low bioavailability, which means they must be delivered via injections[28]. Considering this fact cyclotides are seen as a potential source of new drugs. They are intermediate in size, show specificity similar to “biologics” and at the same time, they have a bioavailability of small molecules. Therefore, they represent a class of new, specific, orally bioavailable, and metabolically stable medications.

Cyclotides are a family of macrocyclic peptides possessing unique structural and biophysical properties. They are ribosomally synthesized by plants and post-translationally modified natural products. They were first discovered by Red Cross workers in Africa in the 1970s. These people noted that the *Lulua* tribe women were given tea made of the *Oldenlandia affinis* plant leaves locally known as *kalata kalata* during childbirth. This decoction accelerated uterine contractions and childbirth. As the plant was boiled and later orally administered, this indicated that the active ingredient was thermally stable and bioavailable[29]. It has been later conclusively determined that the kalata B1 peptide is the primary factor responsible for uterotonic activity[30]. Lately, it has been shown that this peptide is unique among a broad range of peptides because it is resistant to degradation in simulated gastric intestinal digestion assays[31].

Cyclotides in general are considered plant defense peptides. They were discovered in a range of angiosperm plant families like *Rubiaceae, Violaceae, Fabaceae, Solanaceae, Poaceae*, and *Cucurbitaceae*[32]. The peptic cyclotides consist of 28-35 amino acids. The exceptional stability of these peptides is attributed to their uncommon conformation formed by backbone cyclization and three intramolecular disulfate bonds – the cyclic cysteine knot motif (CCNM)[33]. Cyclotides are divided into two main subfamilies depending on the presence of a cis-Pro peptide bond in loop 5. This bond causes a "twist" in the protein backbone (Figure 3). If the given cyclotide possesses this trait it belongs to the *Möbius* subfamily. Cyclotides without the cis-Pro belong to the bracelet family[34].

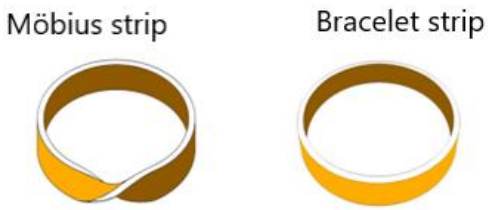

Figure 3: Möbius and bracelet strips (Adapted from Narayani et al, 2020).

The synthetic version of kalata B1 cyclotide (T20K) belongs to the Möbius subfamily. Therefore it contains a *cis*-Pro residue in loop 5 which induces a local 180° backbone twist[35]. The caripe cyclotides belong to the bracelet subfamily and do not possess this structural feature (see Figure 3). *Möbius* peptides are considered to be more potent in interacting with membrane components compared to bracelet-type members[36]. This feature points to different mechanisms of action of these two distinct types.

1.3.1 T20K

Gründemann *et al*. research delved into the correlation between the structure and immunosuppressive properties of cyclotides. They examined the antiproliferative effects of cyclotides on human lymphocytes. They utilized both active (T20K) and inactive (V10K) kalata B1 mutants. The findings demonstrated that cyclotides suppress the ability of T-cells to perform multiple functions and significantly impede the proliferation of immune-competent cells by inhibiting IL-2 biology in multiple locations. This effect was attributed to the stereospecific interaction between cyclotides and their targets[37] . In another related study the effectiveness of the [T20K]kB1 ('T20K') was examined in treating experimental autoimmune encephalomyelitis (EAE) using a Multiple sclerosis (MS) mouse model. Administering the cyclotide orally to the mice resulted in a considerable decrease in EAE symptoms and delayed disease progression. The cyclotide also inhibited lymphocyte proliferation and reduced proinflammatory cytokines, specifically IL-2[38]. Lind *et al*. showed that T20K can modulate the proliferation of anaplastic large cell lymphoma (ALCL). T20K induced apoptosis and inhibited the proliferation of human lymphoma T-cell lines. Treated cells increased STAT5 and p53 signaling but did not alter cytokine levels in lymphoma cells in contrast to IL-2 signaling in normal lymphocytes. Conducted *in vivo* mouse experiments resulted in decreased tumor weight and increased apoptosis when treated with T20K[39].

Gründemann *et al*. was able to synthesize the synthetic cyclotideT20K'. The sequence and the 3D structure of the molecule are presented in Figures 4 and 5, respectively. T20K was synthesized with the use of solid-phase peptide synthesis followed by head-to-tail cyclization and oxidative folding[40]. The peptides were purified by the reversed-phase preparative high-performance liquid chromatography[41].

Figure 4: Sequences of kalata B1 and [T20K]kalata B1 with the use of one letter amino acid code. In red is the point mutation. Jackson et al. 2023[42].

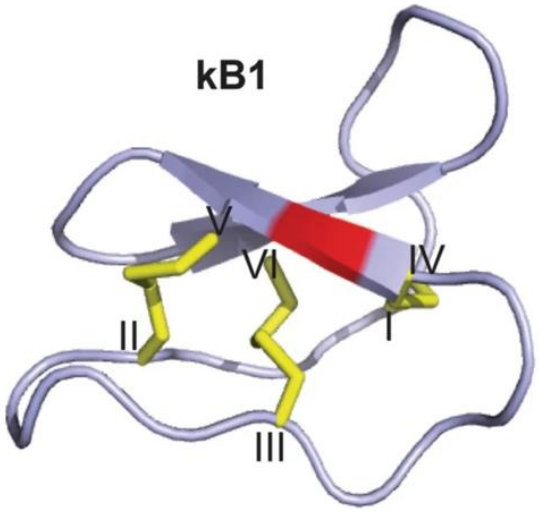

Figure 5: The Kalata B1 protein has three disulfide bonds that form a cystine knot. The [T20K]kB1 mutation causes a variant of this protein that is highlighted in red. Adapted from Jackson et al. 2023[42].

1.3.2 Caripe

Caripe is a type of cyclotide isolated from *Carapichea ipecacuanha* roots. The name ipe-cac-uanha is of Native American origin and might be roughly translated from its Portuguese derivative as the 'roadside vomiting plant'[43]. The mixtures from this plant in the form of herbal preparation of the root extract have been used for over two hundred years as an expectorant or emetic[44]. It was commonly known as 'syrup of ipecac' and was used in Western clinical practice until the late 20th

century. It was later documented that the major alkaloids emetine and cephaeline cause the expectorate and emetic effect[43]. Due to high toxicity, the pure alkaloid emetine was abandoned for use. However, the cyclotides derived from the root extract of ipecac are still of high interest for their potential pharmacological use.

It has been shown that reversed-phase high-performance liquid chromatography (RP-HPLC) applied to a cyclotide-enriched fraction of *C. ipecacuanha* forms further fractions in the eluting

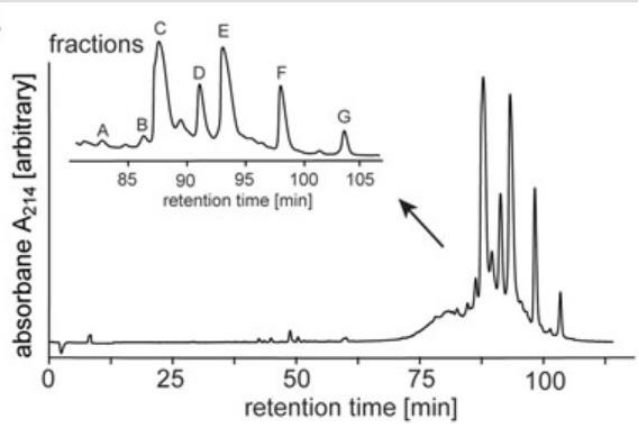

Figure 6:Preparative RP-HPLC A214 chromatograms of crude extract of C. ipecacuanha after cyclotide enrichment via solid-phase extraction. Inset displays the elution profile of the main cyclotide fractions A–G. Adapted from Fahradpour et al.[27]

region. The consecutive letters of the alphabet have been ascribed to these fractions (from A to G). Caripe 11 belongs to fraction C and Caripe 8 belongs to fraction F[44] (see Figure 6).

In a recent study, Taghizadeh *et al.* conducted a screening of plant extracts containing cyclotides[45]. They were interested in the cholecystokinin-2 receptor (CCK2R), a type of G protein-coupled receptor (GPCR). The CCK2R is a receptor found in both peripheral tissues and the central nervous system, making it a potential target for drug development in diseases such as gastrointestinal cancer. They were able to show that extracts from *Oldenlandia affinis*, *Viola tricolor*, and *Carapichea ipecacuanha* all activated the CCK2R. Thereafter they isolated a cyclotide Caripe 11 from the *C. ipecacuanha* extract and further analyzed it. They showed that Caripe 11 is a partial agonist of the CCK2R, with a moderate potency of 8.5µM. It increases basal activity at low concentrations and shifts the potency of cholecystokinin-8 at higher concentrations[45]. Caripe 8 was

found to antagonize the corticotropin-releasing factor type 1 receptor (CRF1R)[44]. Also, a cyclotide extract obtained from the root powder *of C. ipecacuanha* was examined by Fahradpour *et al.* for its ability to modulate the corticotropin-releasing factor type 1 receptor (CRF1R), a type of G protein-coupled receptor (GPCR). The group identified and characterized seven novel cyclotides, including Caripe 8. They showed that this cyclotide antagonizes the CRF1R. At a concentration of 260 nM, caripe 8 reduced the potency of CRF by approximately 4.5-fold acting specifically on the CRF1R[46]. Caripe 8 and 11 are highly promising cyclotides that can be utilized for the creation of drug-like molecules. Their wide range of characteristics makes them a considerable source for developing cyclotide-based ligands.

2 AIM OF THE STUDY

The present study focused on identifying novel therapeutic options for AML. Using a murine in vitro system, we analyzed the sensitivity of cyclotides on AML cell viability. The two AML subtypes harboring either KMT2A-MLLT3 or RUNX1-RUNX1T1 were investigated for their sensitivity towards two types of cyclotides: plant-derived Caripe extract and synthetic peptide T20K. Caripe 8 and Caripe 11 are used for the assays performed in this study.

3 MATERIAL AND METHODS

3.1 AML MURINE *IN VITRO* MODEL

Hematopoietic progenitor cell lines were generated from lineage-negative and lineage-positive selection for c-Kit and Sca-1 mouse bone marrow cells (HPC^{LSK}) [47]. HPC^{LSK} cells were transformed using a retrovirus harboring either pMSCV-KMT2A-MLLT3 IRES (Venus) or pMSCV-RUNX1-RUNX1T19a-IRES (GFP) vectors. The virus was produced by using Phoenix Retroviral Packaging Cells and TurboFect as described recently[48]. The cells were selected for GFP or Venus expression by fluorescence-activated cell sorting analysis (FACS-sorting). Cells used for the assays in this investigation were cultured on 1% agarose-coated 6-well plates with 2-2,5 ml of medium in a 5% CO_2 humidified incubator. Detailed information considering the content of the medium used is presented in Table 1.

Murine cell line	Cell culture media	
KMT2A-MLLT3+ RUNX1-RUNX1T1+	Iscove's Modified Dulbecco's Medium with glutamine (IMDM, Sigma) + 5% FCS + 1% penicillin/streptomycin (Sigma) + 32,5ul/500ml IMDM 1-thiolglycerol (Sigma) +12,5 ng/ml human interleukin-6 (hIL-6) (R&D) +SCF (generated in-house) 1:60	

Table 1:The content of the cell medium used for the murine cell lines.

3.2 CELL VIABILITY ASSAYS

Drug–dose-response curves are generally used to measure and analyze the relationship between an active component's inhibitory capabilities accompanying its respective concentrations[49]. Half maximal inhibitory concentration (IC_{50}) is the concentration at which the compound reaches a 50% reduction in cell viability. The lower the IC_{50} value, the more potent the substance assessed. To establish the IC_{50} of a peptide, the peptide of interest together with $1x10^5$ HPC^{LSK} cells was pipetted in triplicates or duplicates at different concentrations (T20K: 0nM, 300nM, 1µM, 3µM, 10µM, 30µM; Caripe 8: 0nM, 300nM, 1µM, 3µM, 10µM) into uncoated 48- or 96- well plates. The treatment was incubated at 37°C and 5% CO_2. The duration of treatment varied depending on the experiment and peptide of interest.

To measure cell viability after peptide treatment we used the CellTiter-Glo® Luminescent Cell Viability Assay. 100 µl of the cell suspension was transferred to an opaque-walled 96-well plate and 100 µl of the CellTiter-Glo Reagent® (CTG) was added. The plates were covered with aluminum foil and incubated with the CTG reagent for 15 minutes under shaking at 400 rpm on the Thermoshaker (VWR) at 24°C. Subsequently the samples were left for 2 minutes to stabilize the signal. In viable cells, the mitochondria produce adenosine triphosphate (ATP). The used

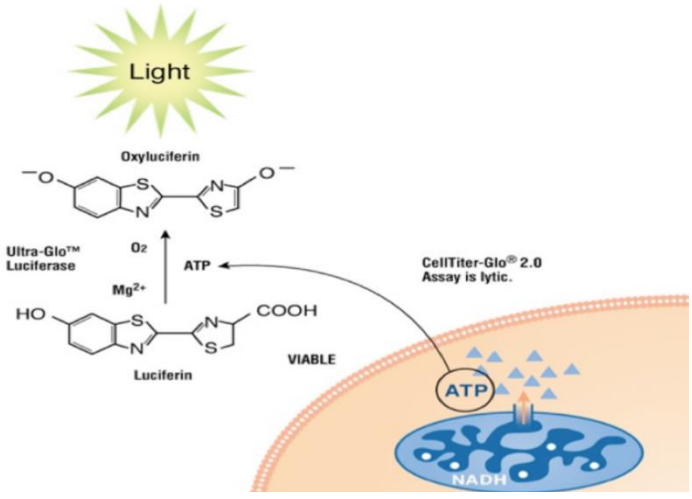

Figure 7: The principle of the cell viability CellTiter-Glo® Luminescent Cell Viability Assay, adapted from CellTiter-Glo®[32].

reagent contains a luciferase molecule that reacts with ATP and forms oxyluciferin. The reaction releases luminescence in the form of light. The luminescence was measured by EnSpire® Multimode Plate Reader (Perkin Elmer, Waltham, MA, USA) or Varioskan™ LUX multimode microplate reader (Thermo Scientific™). The produced luminescence is directly proportional to the number of viable cells. To determine the IC_{50} value, the normalized data was transformed to GraphPad Prism (Version 8). The normalization was performed on the samples with DMSO at a concentration equal to the second-highest concentration of cyclotide used in the experiment. The IC_{50} range was obtained by using interpolation and analysis tools using GraphPad 8.

3.3 EXPERIMENTS USING FLOW CYTOMETRY

Flow cytometry experiments were performed using CytoFLEX S (Beckman Coulter, Inc., Brea, CA, USA) and CytExpert 2.4 software.

3.3.1 Annexin assay

To determine differences in apoptosis among the peptide treatments the samples were analyzed with Annexin V and 7-Aminoactinomycin D (7-AAD). Annexin V binds phosphatidylserine when it is on the outer leaflet of the cell membrane. This event usually occurs during apoptosis and therefore is used as a marker for the process. Annexin V conjugated to a fluorophore enables detection via flow cytometry. 7-AAD is a fluorescent chemical compound with a strong affinity for DNA. 7-AAD can be used for dead cell exclusions and also for samples treated with PE (phycoerythrin)-conjugated antibodies because the emission spectra of 7-AAD and PE can be easily separated on the flow cytometer. For our assays, $1x10^5$ cells were seeded into 48-well uncoated plates. 500µl of peptide-containing media was added to each sample. The cells were treated for four days, and apoptosis was analyzed at day 3 or 4.

For the staining, the 10x Binding Buffer was diluted to 1x in deionized water. 100 µl of cell suspension was transferred to a 96-well uncoated plate. Cells were washed once in the 1x Binding Buffer. Then cells were stained in Annexin V Staining Solution, consisting of 5µl of Antibody in 100µl of Binding Buffer per sample. Cells were incubated for 15 minutes at RT in the dark. Cells were then washed three times in 500 µl Binding Buffer per sample to remove all unspecific bound antibodies. Then, 7-AAD was added, 5µl of antibody in 100µl 1x Binding Buffer per sample. The cells were subjected to flow cytometry analyses using PacBlue for Annexin V and PE-Cy5.5 for 7-AAD.

3.3.2 Surface marker profiling

To investigate the differentiation status of the cells we performed surface marker stainings. An antibody cocktail of surface protein markers was used in a 1:100 dilution in PBS. FC block was added at a 1:100 dilution in PBS to prevent unspecific antibody binding. To set the gating, we utilized the Fluorescence minus one (FMO) control diluted at the same level as the antibody cocktail. The FMO was created by excluding always one antibody from the entire antibody cocktail. FMOs are employed to ensure that certain antibodies do not produce a signal in the wrong channel, regardless of concentration. 100 µl of cell suspension was transferred into a 96-well plate. The plate was centrifuged at 1200 rpm for 5 minutes. The supernatant was removed, and cells were stained with 25 µl of the antibody cocktail. The plate was incubated in the dark at 4°C for 1h. 100µl PBS was added to the plate for washing and then centrifuged at 1200rpm for 5 minutes. The supernatant was removed, and the cells were resuspended in 100 µl of PBS. The plate was analyzed with the Cytoflex S. To evaluate the differentiation status of the cells the antibodies for the following surface markers were used (Table 5).

Surface marker	FACS channel	Targeted cell fraction	Company
Gr-1	BV650	Macrophages	Invitrogen/eBioscienceTM
CD11b	APC-Cy7	Myeloid cells	Invitrogen/eBioscienceTM
c-Kit (CD117)	PE-Cy5	HSCs	eBioscienceTM
Sca-1 (Ly-6A/E)	PE-Cy7	HSCs	eBioscienceTM

Table 2: Lineage and Stem Cell Surface Marker Panel.

FACS gating was set as shown in Figure 8.

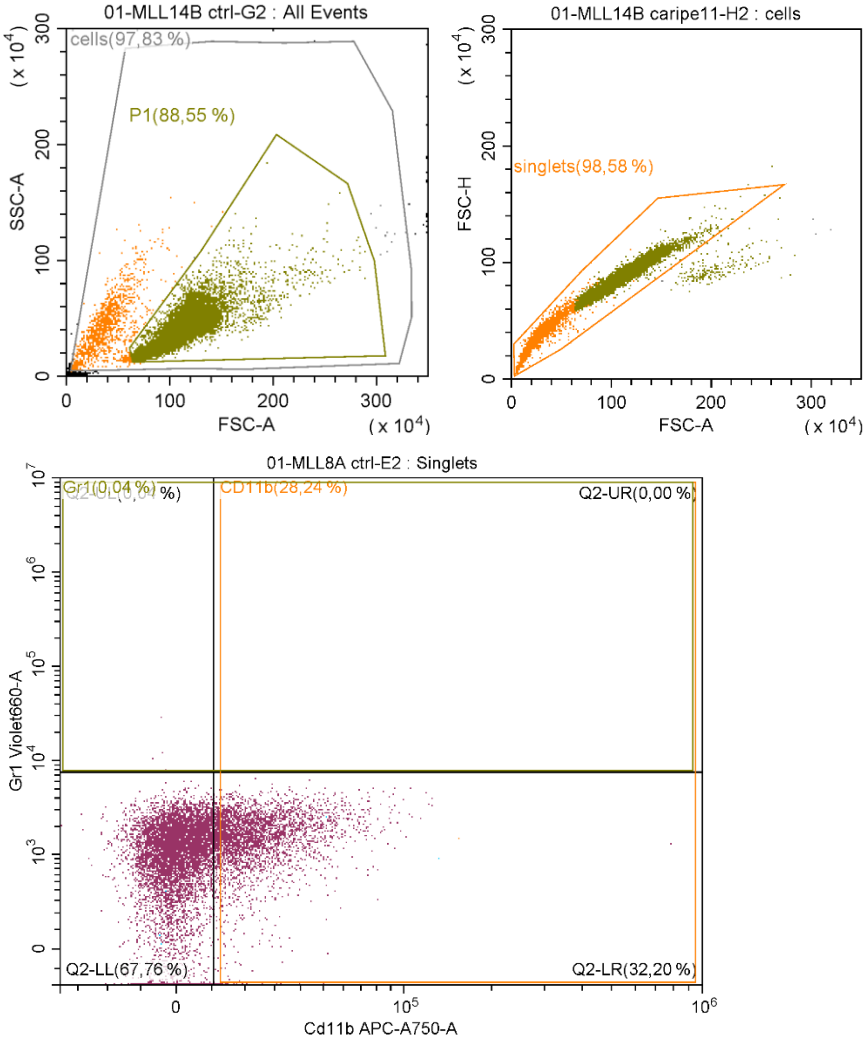

Figure 8: FACS gaiting for surface marker profiling.

3.3.3 Propidium iodide (PI) viability assay

PI is taken up by dead cells as a result of permeabilized membrane and intercalates into the DNA. This enables the detection of a positive signal released by non-viable cells only.

100µl of cell suspension was transferred to 96-well plates and 100µl PI (1:500 in PBS) was added. The plate was analyzed by flow cytometry of the PE channel.

3.4 PROTEIN ASSAYS

Protein has been isolated either from fresh cells or from cell pellets stored at -80°C. Cells were resuspended in RIPA buffer with proteinase inhibitors (PI, Roche). One tablet of PI was dissolved in 1 ml of RIPA buffer. The amount of used PI+RIPA buffer solution was adjusted according to the pellet size in a range between 30 -100µl. The samples were shaken for 30 minutes at 4°C, and subsequently centrifuged at 13000 revolutions per minute (rpm) for 20 minutes at 4°C. The supernatant containing the protein lysate was used for further analysis.

The concentrations of the protein lysates were measured colorimetrically (Pierce™ BCA Protein Assay Kit, Thermo Fisher Scientific) on an EnSpire® Multimode Plate Reader (Perkin Elmer, Waltham, MA, USA) or Varioskan™ LUX multimode microplate reader (Thermo Scientific™). For this analysis, BCA (bicinchoninic acid) 4 mg/ml of BSA in 10 ml water was prepared. Standards were used with the final concentrations of 2, 1.5, 1, 0.75, 0.5, 0.25, and 0 mg/ml.

The standards were pipetted in duplicates into the 96-well plate using 50 µL of deionized water with 5µl of each standard. For the samples, 54 µl of deionized water and 1 µl of protein lysate were used. 200 µl of the Pierce™ BCA Protein Assay Kit (Thermo Fisher Scientific) (solution A and solution B 50:1 ratio) was added to each sample. The plate wrapped in aluminum foil was incubated at 37°C for 20 minutes. Samples were then measured colourimetrically in a plate reader. Protein concentration was calculated, and the same concentration was used from each sample (15µg/µl, 20 µl per sample). Protein lysates were incubated at 95°C with a 4x Laemmli buffer. Subsequently, the samples were loaded onto a 12% sodium dodecyl sulfate-polyacrylamide (SDS-PAGE) gel (see details of the composition of gels in Table 2). Gels were placed in a chamber filled with an SDS running buffer. Gels were exposed to 90 V for 30 minutes following 90 V as long as the proteins were distributed throughout the gel and the loading dye was visible at the very bottom of the gel.

12% resolving gel (ml)		**5% stacking gel (ml)**	
H_2O	6,6	H_2O	5,62

1.5 Tris pH 8.8	5	0.5 Tris pH 6.8	2,5
AcrylBisacryl	8	AcrylBisacryl	1,68
10% SDS	0,2	10% SDS	0,1
10% APS	0,2	10% APS	0,1
TEMED	0,02	TEMED	0,01

Table 3: The composition of resolving and stacking gels used in the assay.

Separated proteins were transferred to ethanol activated Immobilon®-P polyvinylidene difluoride membranes (PVDF; Merck, Cancers 2022, 14, 1554 4 of 16 Darmstadt, Germany) using overnight blotting with 0.2 A for 16 h followed by 0.4 A for 3 h at 4°C. A detailed blotting buffer recipe is presented in Table 3. The membranes were stained with a Ponceau solution (0.1 % Ponceau in 5% acetic acid) to ensure an equal loading amount. Membranes were blocked with a 3% bovine serum albumin (BSA) blocking solution for 1 hour at room temperature (RT). After blocking unspecific proteins, the membranes were incubated in primary antibodies (Table 4) overnight at 4°C. On the next day, the membranes were washed three times for 10 minutes with Py-TBS-T and incubated in a Horseradish peroxidase (HRP)-linked secondary antibody for 1 hour at RT. Membranes were washed three times 10 minutes with Py-TBS-T. A detailed antibody list is presented in Table 4.

The substance	**Amount**
10x Transfer buffer (1.92M Glycine, 250mM Tris)	350 ml
20% Ethanol	700 ml
Deionized water	2450 ml

Table 4: Transfer buffer

Antibodies	**Host**	**Company and Number**	**Dilution**
Bcl-xl	Rabbit	Cell Signaling #2764	1:1000
Cleaved Caspase-3	Rabbit	Cell Signaling #9654S	1:2000

Caspase-3	Rabbit	Cell Signaling #9662	1:1000
ATM	Rabbit	Cell Signaling #2873	1:1000
BCL-6	Rabbit	Cell Signaling #5650	1:2000
Cyclin C	Rabbit	Bethyl Laboratories Inc. #J2711	1:1000
βActin	Mouse	Santa Cruz #69879	1:1000
p53	Mouse	Santa Cruz #126	1:1000
Cytochrome C	Rabbit	Cell Signaling #11940	1:1000

Table 5: Antibodies used for immunoblotting analyses.

The chemiluminescence of the immunoblots was measured with the ChemiDoc™ Imaging System (Bio-Rad, Hercules, CA, USA) after incubation with 20× LumiGLO® Reagent and 20× Peroxide (Cell Signaling Technology, Danvers, MA, USA). The densitometry quantification of the signals was performed with Image Lab 5.2.1. software (Bio-Rad, Berkeley, CA, USA).

The PVDF membranes were subjected to stripping and re-probing. To analyze other target proteins, the antibodies that were bound to the membrane were removed by applying heat. To achieve this, the membrane was microwaved in a heat-resistant container filled with deionized water for 15 minutes at 700 watts. Afterward, it was directly stored in pY-TBST. The membrane was washed three times with pY-TBST, and then blocked before carrying out subsequent steps as per the previous instructions. While stripping, it was ensured that the two target proteins didn't have the same size and, if possible, a different secondary antibody was used.

3.5 STATISTICAL ANALYSIS

All statistical analyses were done using Microsoft 365 and GraphPad Prism software (Graphpad, San Diego, CA). If not stated otherwise, the graphs demonstrate mean ± standard deviation error of the mean (SEM). The difference between the data sets was considered significant when the

obtained p-value was less than 0.05. For Annexin V assays two- way ANOVA multiple was conducted. The p values were considered as follows: *p < .05; **p < .01; ***p < .001.

4 RESULTS

4.1 CARIPE CYCLOTIDES AS NOVEL THERAPEUTIC AVENUES FOR AML

Previous studies suggest that plant-derived circular peptides might be novel possible treatment options for various type of cancer[41,50,51,40]. To find out if Caripe as an example of circular peptide drugs is a valid candidate for the precise treatment of specific AML subtypes, we evaluated its toxicity in this context. We used a novel murine hematopoietic progenitor cell model (HPC^{LSK}) to mimic AML subtypes and to elucidate the effectivity of the Caripe for AML.

We used in the analysis two different fractions of Caripe. As mentioned, before they share a high degree of similarity and only three amino acids are different. The cyclotides have a different sequence in loop 3, which is typically recognized to exhibit the highest sequence variability. Extracting Caripe is challenging and so far, no synthetic compound was established. The restricted availability of the compounds limited the investigation of Caripe 8.

Peptide	Sequence
caripe 8	c-CGESCVFIPCITAAIGCSCKKKVCYRNGVIP
caripe 11	c-CGESCVFIPCISTVIGCSCKKKVCYRNGVIP

Figure 9: The amino acid sequence of Caripe 8 and Caripe 11. Underlined is the sequence of loop 3, in blue six conserved cysteine residues which form three knotted disulfide bonds. Adapted from Falanga at all., 2022.[21]

4.1.1 Drug response curves show sensitivity to Caripe 8 for AML

To determine Caripe potency IC_{50} values, we seeded $5x10^3$ RUNX1-RUNX1T1+ and KMT2A-MLLT3+ HPC^{LSK} cells in increasing concentrations of Caripe 8 (0, 0.3, 1, 3, 10, and 30 µM) and incubated for 24h. Cells were analyzed by using a CellTiter-Glo® Luminescent Cell Viability

Assay. The IC_{50} for KMT2A-MLLT3+ was lower (1.3µM) than the one for RUNX1-RUNX1T1+ (2.4µM) (Figure 10). The obtained IC_{50} values were used as a concentration indication for further viability assays.

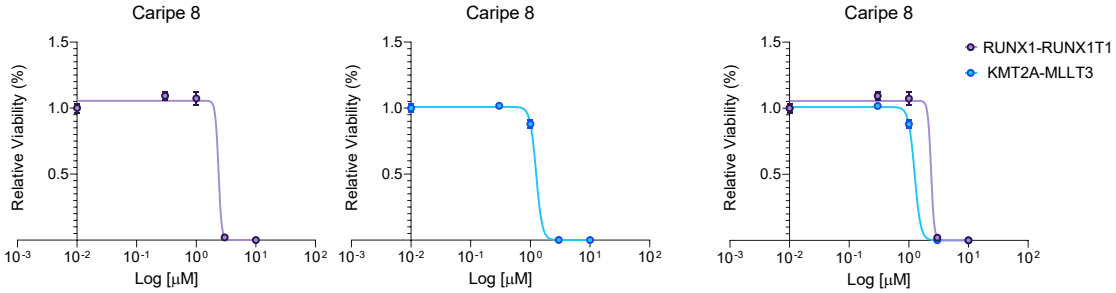

	RUNX1-RUNX1T1	KMT2A-MLLT3
IC50	~ 2.358	1.250

for KMT2A-MLLT3+ cell lines, the response was still visible for biological replicate #3 on day four but not for #1. The trend depicted by analyzing the percentage of living cells matched the trend obtained using the total numbers (Figure 11b). KMT2A-MLLT3+ cell lines showed an even more pronounced effect.

Summarizing we can state that all cell lines respond in a short-term treatment of 1.5µM Caripe 11. A total number of cells decreased in one of the two biological replicates for each oncogene: in the case of RUNX1-RUNX1T1+, biological replicate #1 showed a good response, and in the case of KMT2A-MLLT3+, biological replicate # 2 responded better.

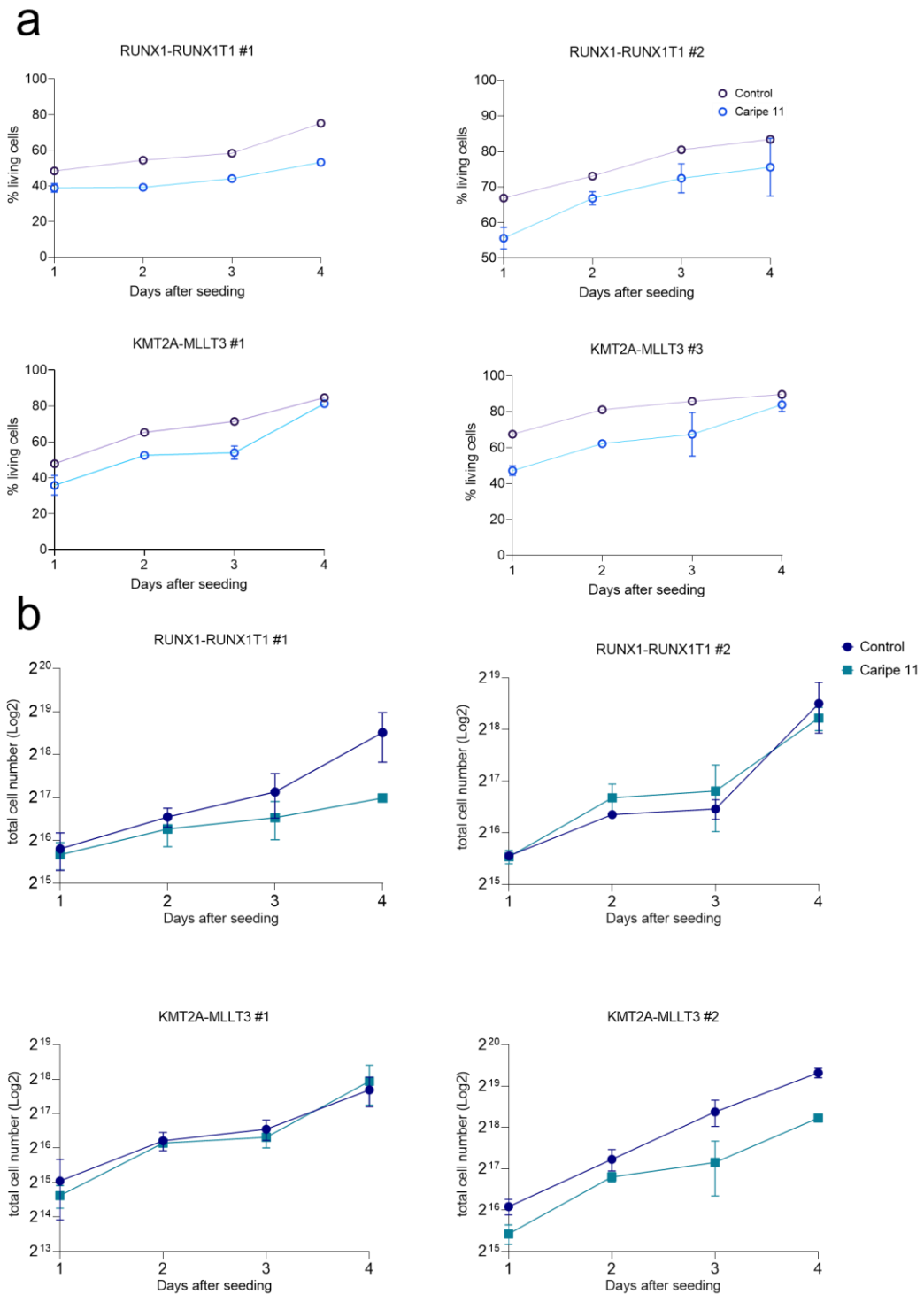

Figure 11a: Curves represent percentages (%) of living cells over four days treatment with 1,5µM Caripe 11 extract of two biological replicates of RUNX1-RUNX1T1 (two technical replicates each) and KMT2A-MLLT3 (two technical replicates each); b: Total number of cells over 4 days treatment with 1,5µM Caripe 11 extract of the two biological replicates of RUNX1-RUNX1T1 (two technical replicate each) and KMT2A-MLLT3 (two technical replicates each) are depicted.

4.1.3 Caripe 11 treatment induces apoptosis but not necrosis

To investigate induction of apoptosis as a potential reason for diminished cell number after Caripe 11 treatment we performed an AnnexinV/7AAD staining. For the analysis we used two channels of FACS: PacBlue for AnnexinV and PE-Cy5.5 for 7-AAD). Living, early apoptotic, late apoptotic and necrotic cell populations are visible on the exemplary dot plots (Figure 12a) depicting the increased number of late apoptotic cells in the treated sample (on the left) compared with the control (on the right). The bar graph in Figure 12b shows the percentage of cells in the distinct categories for two biological replicates of KMT2A-MLLT3+ (on the left) and RUNX1-RUNX1T1+ (on the right). The number of late apoptotic cells was higher, and the number of living cells was lower in each Caripe treated sample. The number of necrotic cells was not significantly different between all samples. In line with the cell viability assays, RUNX1-RUNX1T1+ cell line #1 responded the best as the number of living, early and late apoptotic cells was significantly different compared to the control which was not observed for cell line #2. In the case of KMT2A-MLLT3+ cell lines, there was no significant difference between early apoptotic and necrotic cells, but for both biological replicates, the percentage of late apoptotic cells was significantly increased. Also, biological replicate #2 showed significantly decreased percentages of living cells. This replicate was also the more responsive one in the previous assay.

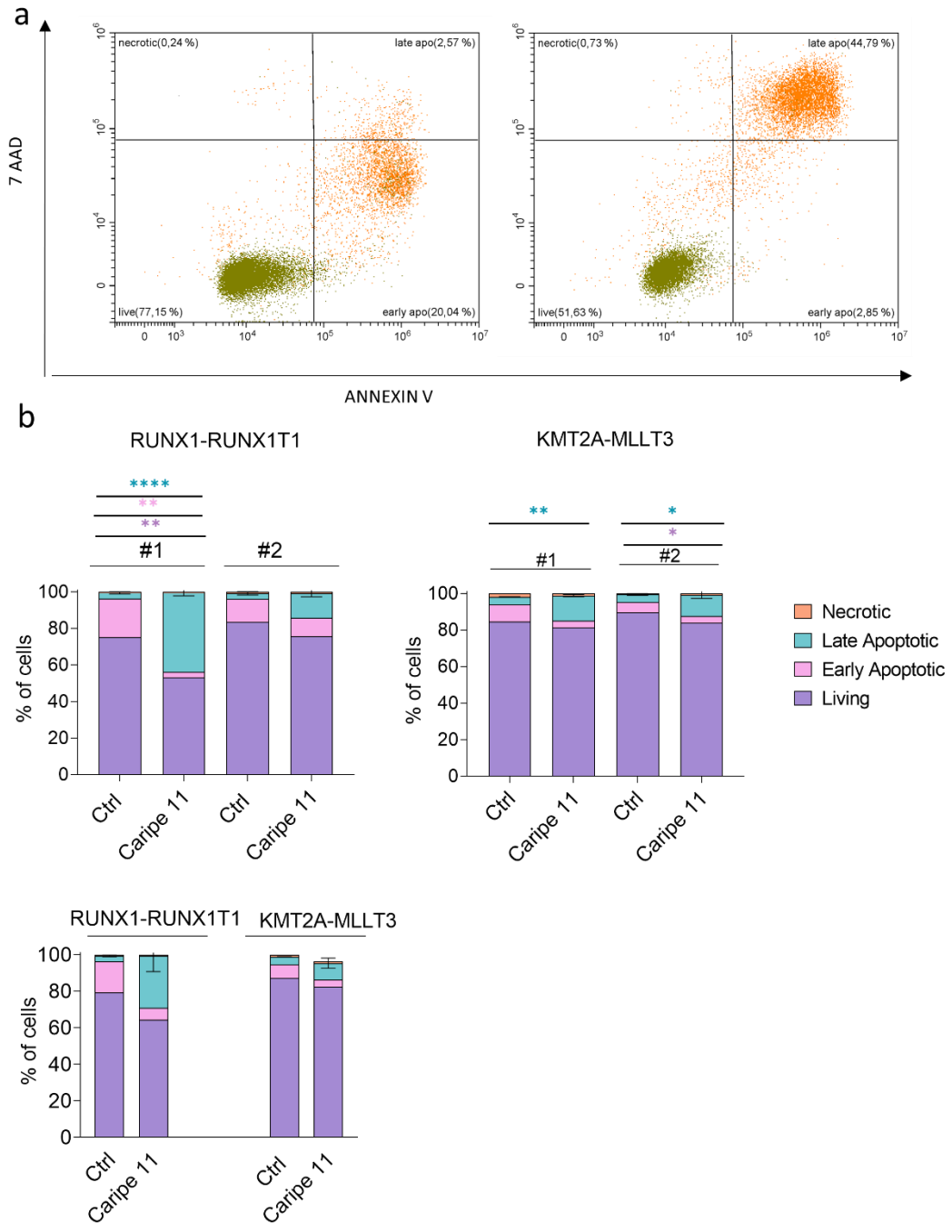

Figure 12a: Blots show an example of the FACS results of Annexin V staining of control and 1,5 µ Caripe treatment samples of RUNX1-RUNX1T1 cell line #1; b: Graphs represent the percentage of necrotic, late apoptotic, early apoptotic, and living cells after four days of treatment of RUNX1-RUNX1T1 and KMT2A-MLLT3 cell lines with 1,5 µM Caripe treatment.

The data indicate that Caripe 11 induces apoptotic processes in AML cells.

4.1.4 Caripe 11 treatment does not induce cell differentiation

To determine a potential induction of cell differentiation we performed surface marker profiling of the AML cells after four days of Caripe treatment. Cluster of differentiation 11b (CD11b) is known as a marker for myeloid-derived suppressor cells[52]. The Gr-1 antigen is primarily a marker of myeloid differentiation. In the bone marrow the level of Gr-1 expression is low on immature myeloblasts and increases as the myeloid cells mature to granulocytes. Therefore, CD11b and Gr-1 were used as a myeloid lineage marker in this assay. The percentage of Gr-1 positive cells was very low and for all the samples was between 0,03-0,26%. This is depicted by the exemplary dot plots from FACS staining of Gr-1 positive cells (two upper quadrants) for untreated (Figure 13a, left) and treated samples (Figure 13a, right). Percentages of CD11b+ cells in RUNX1-RUNX1T1+ and KMT2A-MLLT3+ cells were different between the biological replicates but not between the treated and untreated samples. For RUNX1-RUNX1T1+ was between 65-80% for the control and 66-70 for the treated samples for #1 (Figure 13b upper left) and between 24-29% for the control and 21-23% for the #2 (Figure 13b upper right). For the cell line harboring KMT2A-MLLT3 mutation CD11b+ cells were between 24-29% for all the samples of #1(Figure 13b lower left)and between 83 and 85% for #2 (Figure 13b, lower right). We also checked Mean Fluorescence Intensity (MFI) of CD11b+ and Gr-1 and in this case the data was similar for the control and Caripe 11 treated samples for each biological replicate (Figure 13c).

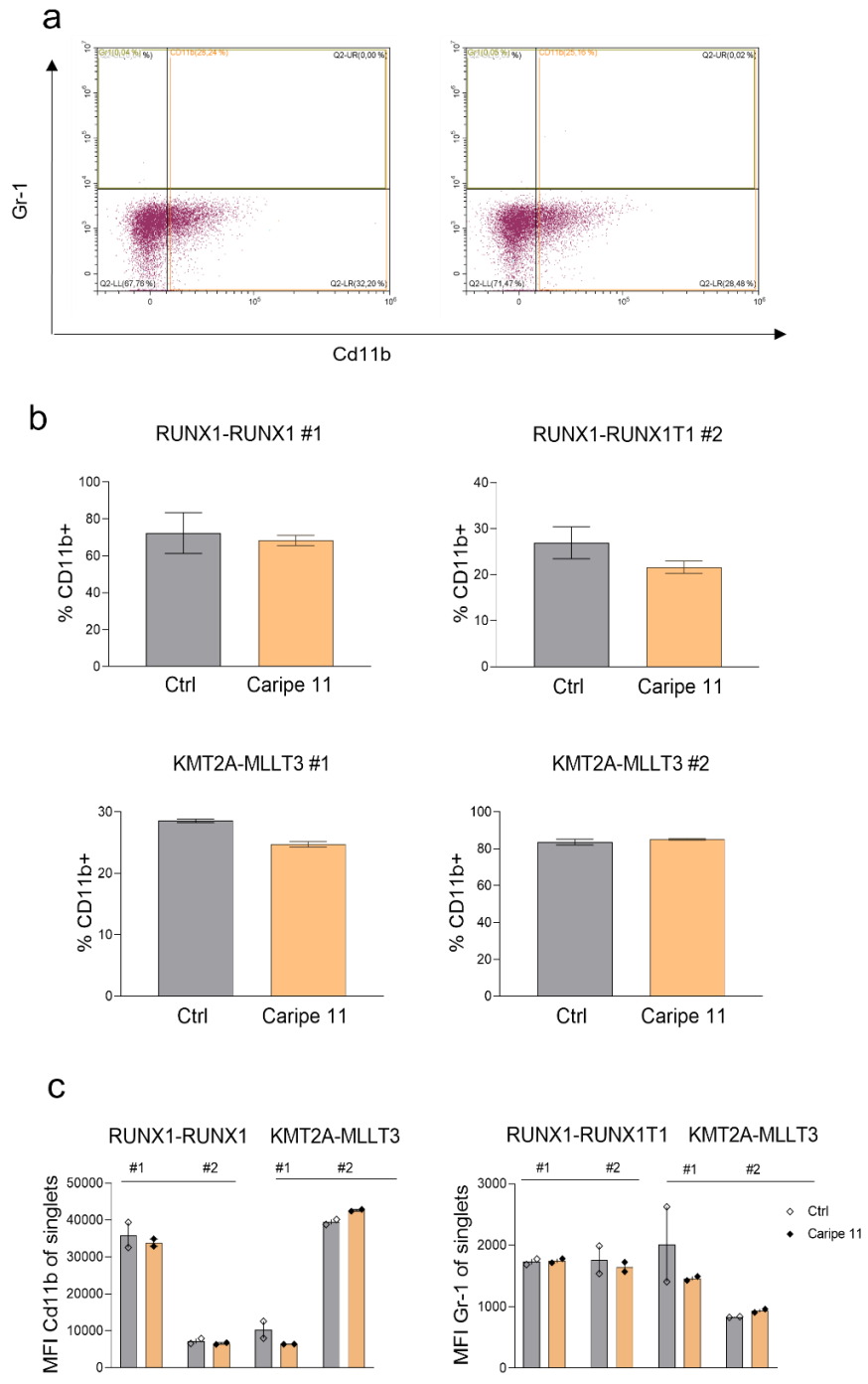

Figure 13a: Example of dot plot analysis of Cd11b+ and Gr1+ cells of KMT2A-MLLT3 # 1 of samples from the control and 1,5 µM Caripe 11 extract treatment after four days; b: Percentage of CD11b+ cells in two biological replicates of RUNX1-RUNX1T1 (3 technical replicates) and KMT2A-MLLT3 (3 technical replicates); c: Mean Fluorescence Intensity (MFI) of Myeloid Lineage Markers CD11b and Gr1 for 2 biological replicates of RUNX1-RUNX1T1 (n=3) and two biological replicates of KMT2A-MLLT3 (n=3).

C-kit is a receptor tyrosine kinase and is present in various cell types such as HSCs, mast cells, germ cells, and melanocytes. C-kit is important for HSCs lodging to the bone marrow "niche"[53]. Sca-1 (Ly-6 A/E) is a cell surface protein found on the surface of hematopoietic, mammary gland, cardiac, and mesenchymal stem cells. It is linked to glycosylphosphatidylinositol (GPI), and studies have shown that it is essential for the normal activity of HSCs and may play a role in their self-renewal. Moreover, it is believed that Sca-1 may be involved in the function of integrins in HSCs[53]. Both sca-1 and c-kit, were used in the investigation as stem cell markers. As it is shown in Figure 15 the treated and untreated cells did not depict major differences in the levels of the surface markers. As depicted in the upper row of Figure 15 upon treatment, the percentage of c-kit positive cells did not change for both biological replicates of RUNX1-RUNX1T1+ and KMT2A-MLLT3+ cell lines and stayed between 99-100%. Upon treatment also the percentage of ca-1 positive cells was very similar and did not change (Figure 14b). Between 99-100% of RUNX1-RUNX1T1+ cells and KMT2A-MLLT3+ #1 cells were sca-1+. For biological replicate KMT2A-MLLT3+ #2 cell line the percentage of sca-1 positive cells was between 87-90%. These results support the conclusion that Caripe treatment does not cause myeloid differentiation.

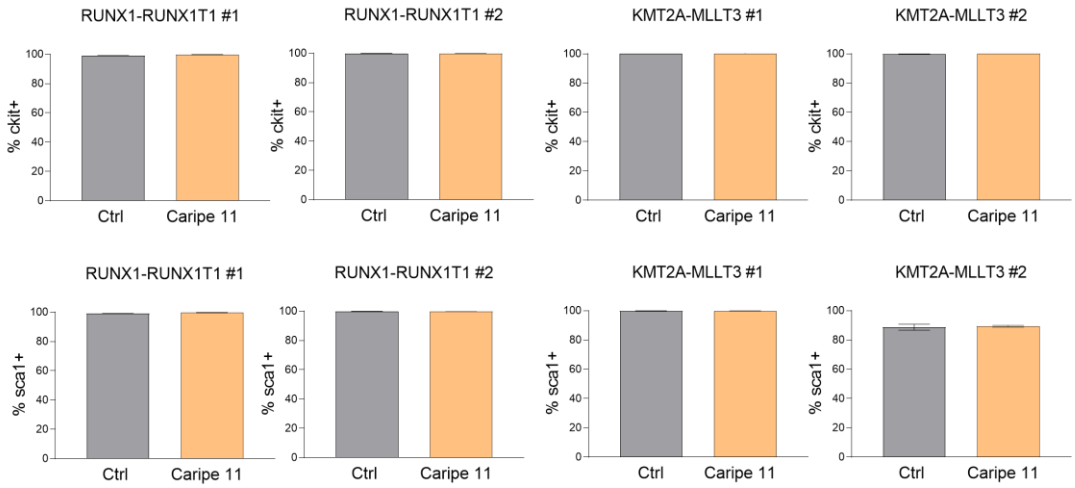

Figure 14: Percentage of c-kit positive cells for two biological replicates of RUNX1-RUNX1T1 (with 3 technical replicates) and KMT2A-MLLT3 (with 3 technical replicates) (upper row), The lower raw presents the percentage of sca1 positive cells for two biological replicates of RUNX1-RUNX1T1 (with 3 technical replicates) and KMT2A-MLLT3.

4.2 SYNTHETIC CYCLOTIDE T20K

4.2.1 Drug response curves of T20K treated cell lines

T20K has been previously shown to be a novel therapy for lymphoid leukemia. We here aimed to investigate the effects of the synthetic compound T20K on AML cells. We seeded $5x10^3$ cells in a 96-well plate. We added different concentrations of T20K (0, 0.3, 1, 3, 10, 30µl). Again, two biological replicates were used to minimize the amount of compound used. The results are presented in Figure 15.

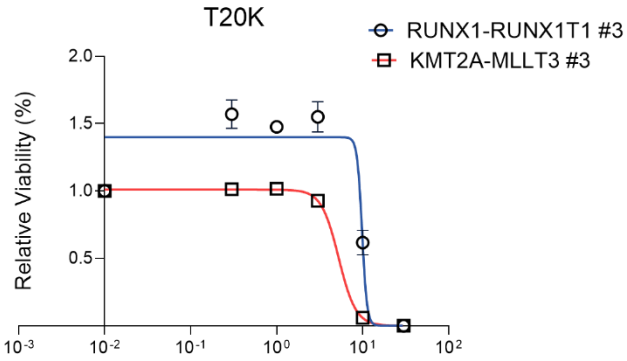

	RUNX1-RUNX1T1 #3	KMT2A-MLLT3 #3
IC50	~ 9.845	5.255

Figure 15: IC_{50} results for the RUNX1-RUNX1T1 and KMT2A-MLLT3 in three technical replicates for each cell line, treated with various concentrations of T20K peptide up to 30µM concentration. Below calculated values of IC_{50}s.

The IC_{50} value for the RUNX1-RUNX1T1+ cells was determined with lower certainty and was found to be almost 10µM. On the other hand, the IC_{50} value for the cell line with KMT2A-MLLT3+ mutation was specified to be 5.25µM. Due to these variations two concentrations of T20K were used for further analysis of the RUNX1-RUNX1T1+ cell line, one matching the IC_{50} value and the other corresponding to the value determined for the KMT2A-MLLT3+ cell line (5 and 10µM).

4.2.2 T20K treatment lowered the cell viability

We first analyzed the viability of the cell lines expressing RUNX1-RUNX1T1+ or KMT2A-MLLT3+ oncogenes when treated with T20K. $1x10^5$ cells were seeded into an uncoated 48-well plate and T20K medium was added. Living cells were counted every day for four days by FACS.

T20K treatment of the cell lines expressing KMT2A-MLLT3 mutation caused a decrease in cell viability and cell number in only one biological replicate (#3) (Figure 16a). The effect was not visible in replicate #1 (Figure 16b). Replicate #1 appeared to require a higher dose of T20K. These results seem to indicate that the biological replicates used were heterogeneous.

For the cells expressing RUNX1-RUNX1T1 mutation, the biological replicates responded similarly (Figure 16c and d). Using 10µM killed all RUNX1-RUNX1T1+ cells after two (replicate #1) or four (replicate #2) days of T20K treatment. These results indicated that this dose, although indicated by $IC_{50,}$ was too high. 5µM T20K treatment resulted in the death of almost all of the cells for biological replicate #1, and biological replicate #2 responded significantly less (37% living cells) upon treatment compared to the DMSO control (60% living cells).

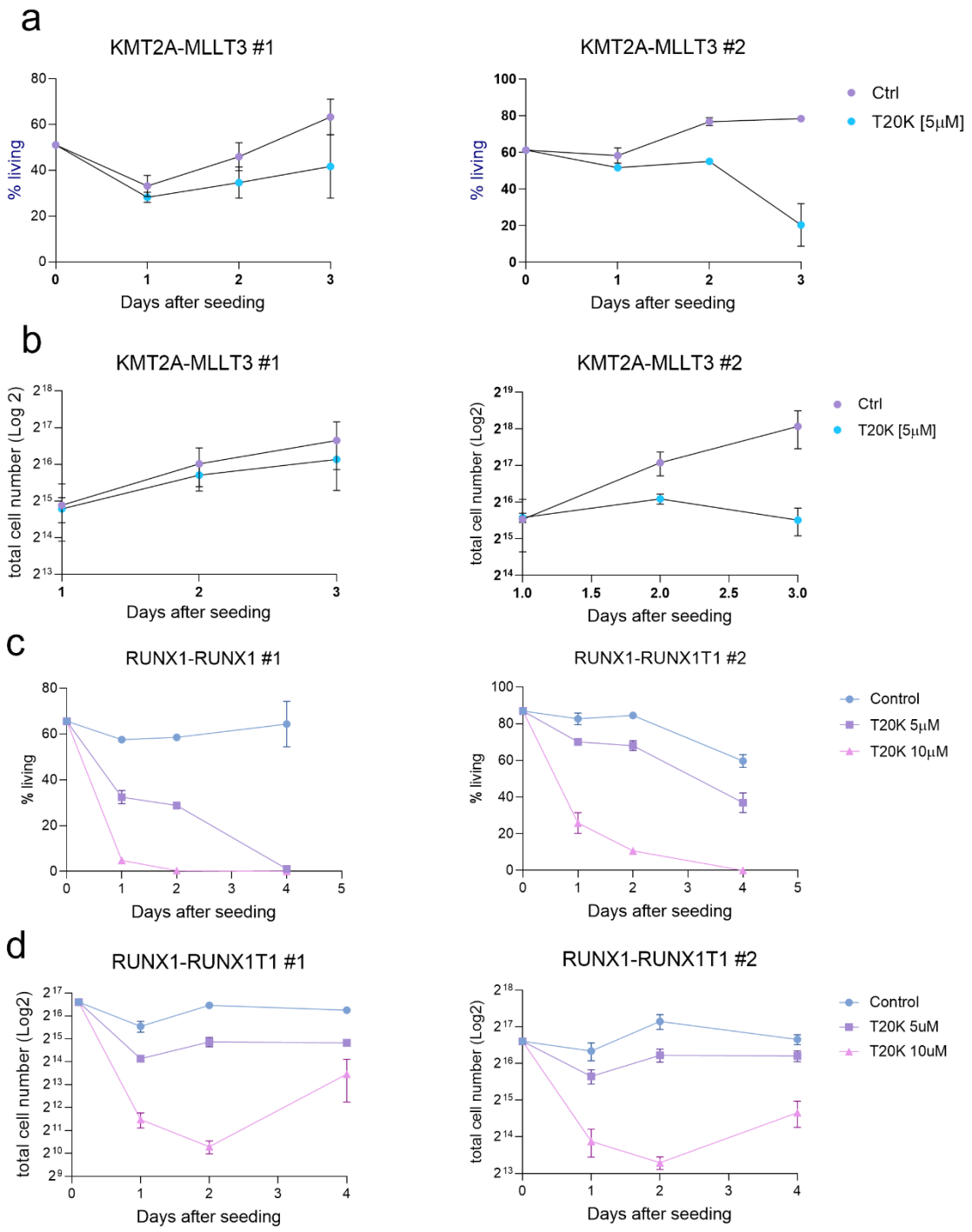

Figure 16a: Percentages (%) of living cells are depicted over the three days treatment with 5µM T20K peptide of the two biological replicates of KMT2A-MLLT3 (two technical replicates each); b: Total number of cells during the 3 days treatment with 5µM T20K peptide of the two biological replicates of KMT2A-MLLT3 are shown (two technical

*replicates each); c: Percentages (%) of leaving cells are depicted over the three days treatment with 5µM and 10µM T20K peptide of the two biological replicates of RUNX1-RUNX1T1 (two technical replicates each); d: Total number of cells over the three days treatment with 5µM and 10µM T20K peptide of the two biological replicates of RUNX1-RUNX1T1*are shown *(two technical replicates each).*

4.2.3 T20K treatment induces apoptosis and necrosis

Since the viability of the cells treated with T20K went down with each day for almost all of the cell lines the increased apoptosis was proven via Annexin V assay. The bar graph in Figure 18a shows the percentage of cells in the distinct categories for two biological replicates of KMT2A-MLLT3+ (on the left) and RUNX1-RUNX1T1+ lines (on the right). A noticeable difference in the percentage of living cells for both KMT2A-MLLT3+ cell lines validated the results from the experiment. In addition, both biological replicates had a significant increase in the percentage of necrotic cells. No significant difference was observed in the late and early apoptotic cells upon treatment.

Figure 17c depicts the flow cytometry results of the control, 5 µM and 10µM treatments to exemplary show the distribution of cells into the four separate groups of cell viability using the annexin V staining: necrotic, late apoptotic, early apoptotic, and live cells. We noticed significant differences in the number of apoptotic cells.

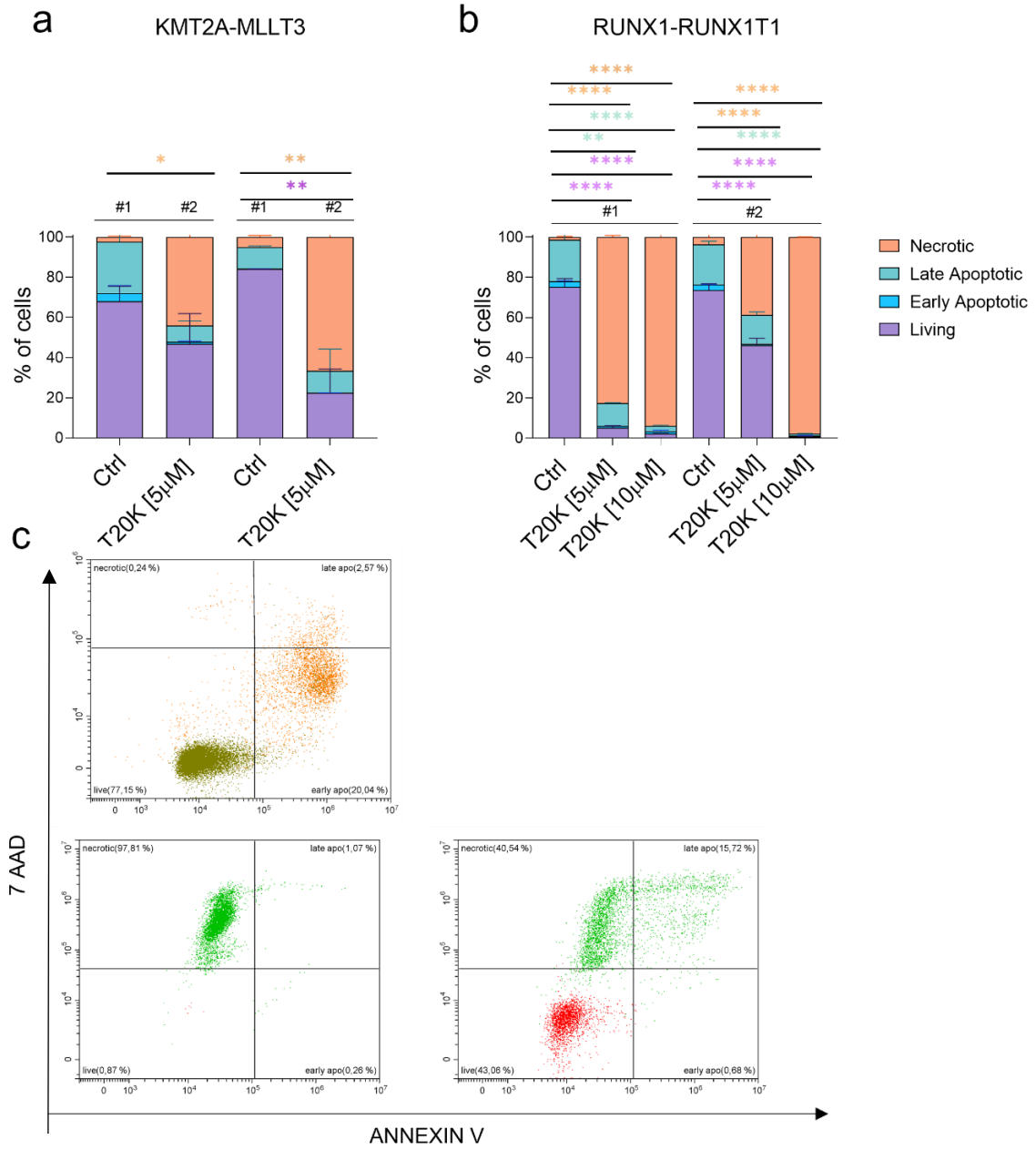

Figure 17a: Bar graphs represent the percentage of necrotic, late apoptotic, early apoptotic, and living cells after 48 hours treatment of KMT2A-MLLT3 cell lines with 5µM T20K peptide; b: bar graphs represent the percentage of necrotic, late apoptotic, early apoptotic, and living cells after 48 hours treatment of RUNX1-RUNX1T1 cell lines with 5µM and 10µM T20K peptide; c: FACS dot plots depicting an example of the results of Annexin V and 7AAD staining of control upper panel), 5µM (lower right panel) and 10µM (lower left) T20K peptide treatment samples of a RUNX1-RUNX1T1 cell line.

In the RUNX1-RUNX1T1+ cell lines, a significant decrease in the percentage of living cells was observed upon T20K treatment which is again in line with the result from Figure 17. There was no significant difference observed in terms of early apoptotic cells among any of the groups. Late apoptotic cells showed considerably higher percentages in the treated samples as compared to the controls, except for the 5µM treatment in biological replicate #2 where the difference was not significant. Necrotic cells were significantly increased in all samples treated with T20K compared to the controls.

4.2.4 T20K treatment alters apoptosis-related proteins

The observed difference in the number of apoptotic and necrotic cells directed the interest in certain apoptosis-related protein levels in T20K treated cells. $1x10^6$ cells were seeded into the well of a 6-well plate and 2 ml of plain, 5µM, or 10µM medium was added. After 48 hours of incubation, the cells were harvested, and samples were prepared for Western blotting. The Western blot results have been quantified and normalized to a β-Actin control (Figure 18).
Knowing that Caspase-3 is a marker of programmed cell death and the levels of cleaved Caspase-3 have been linked to cancer progression in tumor specimens[54] we checked the levels in our samples. Surprisingly, we observed that samples treated with 5µM T20K exhibited lower levels of cleaved Caspase-3 and higher level of Caspase 3, in 10µM T20K treated samples the trend was the same.

The next checked protein was Cyclin C. The Cyclin C/CDK8 complex plays a crucial role in the regulation of transcription, mitochondrial dynamics, apoptosis, and cell cycle progression[55]. Our results showed an increase in the amount of Cyclin C in 5µM T20K treated samples but a decrease in the 10µM T20K treated samples.

Another important regulator of apoptosis is the anti-apoptotic protein Bcl-2. Bcl-2 exerts a survival function in response to a wide range of apoptotic stimuli through inhibition of mitochondrial

cytochrome C release[38]. In the analyzed samples the level of Bcl-2 first increased and later decrease, and Cytochrome C increased upon 5 μM T20K and with higher dosage decreased.

The B-cell lymphoma 6 (BCL-6) gene is responsible for regulating transcription and is known as a proto-oncogene. It plays a vital role in the innate and adaptive immune system, as well as in lymphoid neoplasms[56]. BCL-6 was observed to be induced by a variety of cellular stresses, including exposure to chemotherapy, which is thought to enable cells to tolerate stressors such as cytotoxic agents[57]. The 5μM T20K treatment increased the BCL-6 level what can indicate its cytotoxic effect.

Bcl-xL is another crucial player in preventing apoptosis through heterodimerization with apoptotic proteins, like Bax and Bak, inhibiting its apoptotic effect[58]. Interestingly, in the analyzed samples, Bcl-xL was the highest in the 5 μM treatment.

Next, we also checked the level of ataxia telangiectasia mutated kinase (ATM) in our treated samples. ATM is a serine/threonine protein kinase best known for its role in DNA repair signaling in response to DNA double-strand breaks. When double breaks occur, the sensor complex recruits ATM to sites of DNA damage. ATM then signals to numerous effector proteins, leading to cellular responses including regulation of DNA repair, cell cycle progression, apoptosis, and gene transcription[59]. Interestingly, the analyzed samples showed that the ATM level was lowest in the 5μM T20K treated samples compared to the controls.

Finally, we checked p53 which was already been described to be upregulated upon T20K treatment in ALCL samples. p53 is a tumor suppressor protein that plays a pivotal role in the cellular response to DNA damage and other genomic aberrations. Activation of p53 can lead to either cell cycle arrest and DNA repair or apoptosis[60]. In our samples the level of p53 was the highest in the 5μM T20K samples.

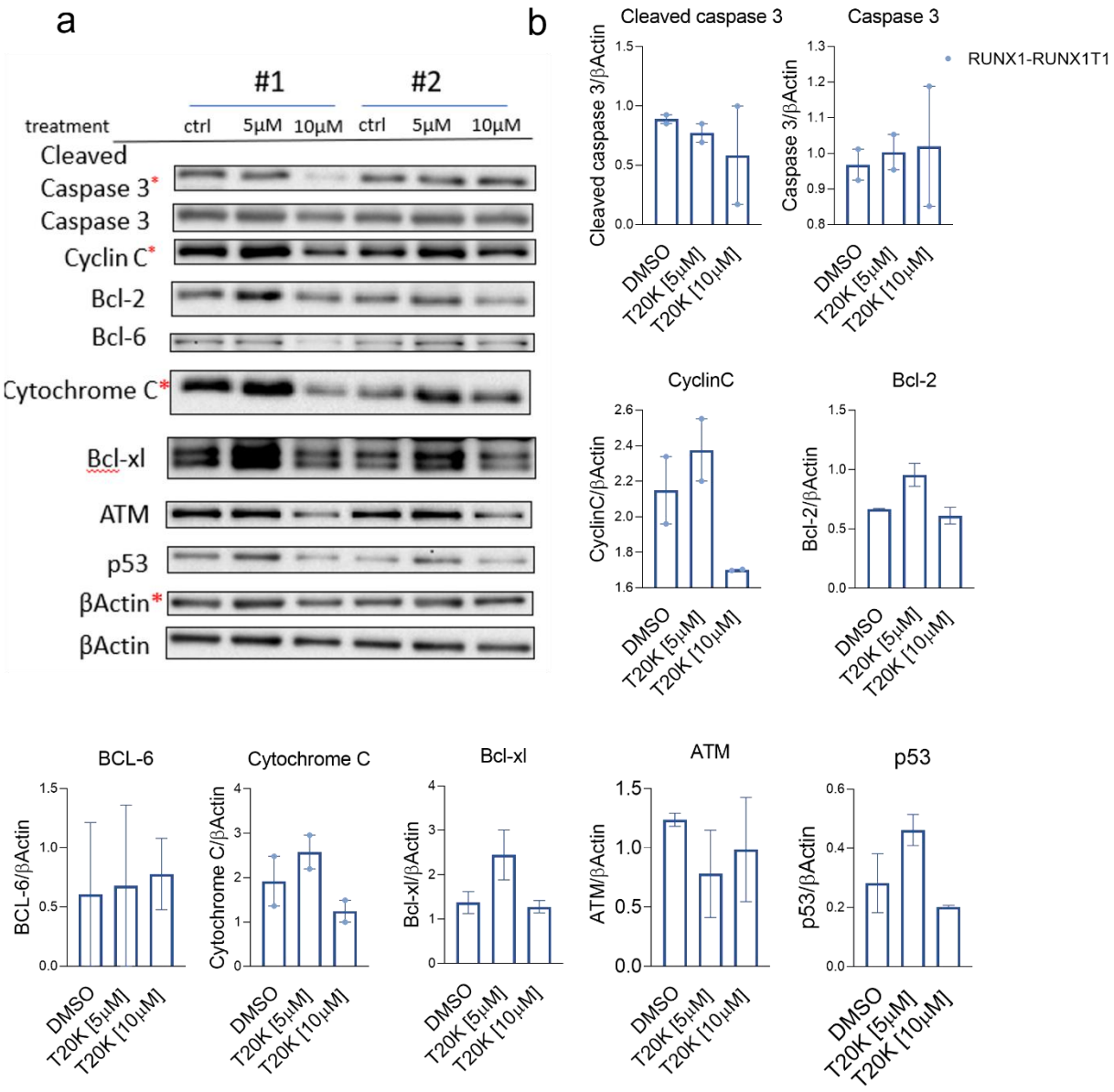

Figure 18a: depicts the results of immunoblot analysis of RUNX1-RUNX1T1+ cells treated with DMOS, 5μM, and 10μM T20K peptide for 48 hours; b: the relative abundance of Cleaved caspse3, Cyclin C, Cytochrome C, BCL-2, ATM, p53, Bcl-xl, and Caspase 3 proteins was normalized to βActin.

The Western blot results elucidate that the cells harboring RUNX1-RUNX1T1 mutation treated with 1,5µM T20K alters apoptosis related proteins.

5 DISCUSSION

5.1 ANTICANCER BIOACTIVITY OF CARIPE AND T20K

So far various cancer cell lines have been studied to determine the effectiveness of cyclotides in fighting cancer. However, nothing is known about the effectiveness of Caripe and T20K on AML cells. Out of 69 different cyclotides tested, it has been found that they possess a remarkable ability to induce toxicity in cancerous cells and solid tumors, including those that resist traditional chemotherapy treatments[51]. The IC_{50} values obtained from these studies ranged from 0.1-0.3μM for Cycloviolacin O2 against RPMI-8226/s (B lymphocytes), RPMI-8226/Dox40, RPMI-8226/LR-5, CCRF-CEM (T lymphoblast), CCRF-CEM/VM-1, NCI-H69 (pancreas), NCI-H69/AR, U-937GTB (pleural effusion), U-937Vcr, and ACH cell lines to 10-46.62 μM for Varv D against MDA-MB-231(breast; mammary gland), A549 (lung), DU145 (prostate), U251(glioblastoma), and BEL-74023(liver)[51]. However, nothing is known about the effectiveness of Caripe and T20K on AML cells. In our study, murine AML cell lines were utilized to first evaluate the efficacy of Caripe extracts. The results displayed a low IC_{50} value of 2.4μM for the cell line expressing the RUNX1-RUNX1T1 mutation, and an even lower value of 1.3μM for the cell line expressing the KMT2A-MLLT3 mutation.

In a previous study, concentrations of Caripe 11 ≤30 μM did not have significant effects, but a concentration of 100 μM slightly decreased the viability of human embryonic kidney (HEK) cells[45].

Considering the above-presented results and IC_{50} obtained in our investigation with the use of the murine cell lines and both type of cyclonites further and deeper analysis regarding the possible treatment of AML patients is needed. To gain a better understanding of the transcriptional targets in AML treatment, it would be helpful to analyze changes in signaling through transcriptomic analysis. By comparing the expression of deregulated genes between treated and control groups, pathway analysis can uncover which cellular and molecular processes are deregulated. This data

can provide a broader mechanistic explanation for the results. In addition, the results of Caripe 11 and T20K analysis should be validated in human AML cell lines harboring the same mutations. This can be achieved by examining cell viability, proliferation rates, and colony-forming potential in methylcellulose.

T20K already showed promising results when used against human lymphoma T-cell lines. It induced apoptosis and proliferation arrest, partly through increased STAT5 and p53 signaling. It did not alter cytokine levels in lymphoma cells and *in vivo* mouse experiments reveal decreased tumor weight and increased apoptosis. The results were obtained by using 4μM of T20K[40]. In our study, we obtained IC_{50} values of 9.8μM for RUNX1-RUNX1T1+ cells and 3μM for KMT2A-MLLT3+ cells. Our further viability assays indicated that the concentration of T20K used could be lower than 5μM. It seems beneficial to repeat the experiments and define the IC_{50} values for human AML cell lines.

5.2 Cell viability after Caripe and T20K treatments

Cell viability was assessed for two different biological replicates expressing the KMT2A-MLLT3 mutation upon Caripe 11 treatment. The viability was lowered in both cell lines, but the effect was more pronounced in biological replicate #3. The viability of biological replicate #1 was not significantly different from one of the control treatments, which suggested that the concentration of T20K for the treatment used (1.5μM) has no cytotoxic effect and the experiment should be repeated using the higher concentration of Caripe. In line, different responsiveness was observed in the case of the cell lines expressing the RUNX-RUNX1T1 mutation with the more responsive biological replicate #1. The initial measurement showed a noticeable cytotoxic effect after 24 hours. However, when fresh Caripe 11 medium was added on the second day, the effect on day three was not as clear as on the first day. These results indicate that the most significant changes occur in a rapid manner, and further analysis should be conducted within 12 or 24 hours of treatment. The analysis was limited due to the low number of biological and technical replicates

used, so the experiment should be repeated with these factors in mind. Increasing the molarity of Caripe 11 to 2-3µM could also potentially yield interesting outcomes, since some biological replicates are less sensitive to the treatment than others.

RUNX-RUNX1T1+ cell lines were treated with 5 and 10µM T20K. However, 10µM T20Kturned out to be cytotoxic for both biological replicates up to four days of treatment. For biological replicate #1, even the concentration of 5µM T20K was cytotoxic at day four. This suggests that the IC_{50} values are different for the individual biological replicates and that the cell lines themselves are very heterogenous, meaning that some of the replicates are more sensitive than others. This is consistent with other studies conducted in our laboratory, where this replicate was more responsive to treatments (data not published). Transcriptomic data from those cell lines validated a high heterogeneity already in an untreated condition (data not shown). For further analysis, cell lines with the RUNX-RUNX1T1 mutation should be treated with a lower concentration of this cyclotide. It also seems reasonable to evaluate more biological replicates. Considering all the above results, tests with Caripe 11 for AML cell lines should be continued, as they remain promising.

5.3 APOPTOSIS IS INDUCED BY BOTH CYCLOTIDE TYPES

In response to T20K treatment, KMT2A-MLLT3+ cell lines exhibited a notable increase in necrotic cells in both replicates. Late apoptotic cells were significantly increased upon treatment, except for KMT2A-MLLT3+ #2 replicate with 5µM treatment. All T20K-treated samples had more necrotic cells than the controls. The data obtained was in accordance with a previously published study, where an apoptotic and necrotic function of the cyclotide T20K on ALK-positive as well as ALK-negative malignant cells has been shown[40].

In our investigation Caripe treatment led to more late apoptotic cells and fewer living cells in all samples, indicating apoptotic processes similar to T20K treatment. However, necrotic cell numbers were similar across all samples. KMT2A-MLLT3+ cells showed no significant difference in early apoptotic and necrotic cells, but both replicates had more late apoptotic cells. Again, cell line heterogeneity could be observed, biological replicate #2 had fewer living cells and was more

responsive. Galanga *et al.* reported that a 10µM mixture of all Caripe peptides caused a reduction in T cell proliferation. Likewise, the incubation of Caripe 11 at a concentration of 10µM resulted in a significant increase in the number of apoptotic cells[36]. Therefore, it would be of great interest to test higher than 1,5µM concentrations of Caripe 11 on untransformed cells and analyze possible effects.

5.4 CARIPE 11 DOES NOT INDUCE DIFFERENTIATION

A variety of agents stimulate differentiation of the cell lines isolated from leukemic patients.1,25-dihydroxyvitamin D3 (1,25D) is capable of inducing in vitro monocyte/macrophage differentiation of myeloid leukemic cells, clinical trials have been performed to estimate its potential to treat patients with AML[61,62]. In our study, we checked if Caripe 11 treatment caused myeloid differentiation in our AML cell lines. By using CD11b, c-kit, and Sca-1 markers we checked the differentiation state of the cells upon treatment, but no differences were seen. In our study, Caripe did not induce differentiation in KMT2A-MLLT3+ or RUNX1-RUNX1T1+ cells.

5.5 T20K TREATMENT INDUCES APOPTOSIS IN AML

Li et al. had shown that Cyclin C acts as a tumor suppressor, but its effectiveness is reduced when there is a loss of one copy of the gene[63]. It is also known that when oxidative stress occurs within mammalian cells, a small portion of Cyclin C is released from the nucleus into the cytosol where it interacts with and activates Drp1, a mitochondrial GTPase. This process leads to mitochondrial fission, indicating that Cyclin C is responsible for inducing fragmentation through the fission machinery[64]. Current studies have shown that while HeLa cells display Cyclin C mitochondrial relocalization and fragmentation upon oxidative stress, the human osteosarcoma U2O2 cells exhibit nuclear Cyclin C release and mitochondrial localization without inducing fragmentation[64].

This indicates that Cyclin C's control over mitochondrial dynamics may differ depending on the cancer type being examined. In our study, T20K treatment increased Cyclin C levels which correlate with increased apoptosis. The exact mechanism which is incorporated into the process is not clear, and further studies are needed regarding this matter. Checking the localization of Cyclin C could indicate if the relocalisation of it takes place upon T20K treatment.

As mentioned before Cytochrome C plays a crucial role in activating Bax, leading to mitochondrial fragmentation and apoptosis. It is a reliable and sensitive marker for therapy-induced cell death, making it an important indicator for apoptosis. However, Barczyk et al. showed that elevated levels of serum Cytochrome C indicate a negative prognosis in cancer therapy[65]. The translocation of Cytochrome C to the cytoplasm is a critical step in initiating the apoptosome-dependent apoptotic cascade, highlighting the significance of serum Cytochrome C levels as a marker of apoptotic cell death[65]. In our study, the Cytochrome C was the highest in the case of 5μM treatment further supporting increased apoptosis observed after the T20K treatment.

Apoptosis is a programmed cell death process controlled by BCL-2 proteins, including Bcl-xL and Bcl-2. Pro-apoptotic ones can be effectors or BH3-only proteins. Anti-apoptotic proteins, like BCL-2 itself, are often overexpressed in malignant cells, increasing their drug resistance[66]. In the samples analyzed, the level of Bcl-2 protein was found to be higher in the samples treated with 5 μM T20K compared to the controls. This does not agree with the results obtained by Lind *et al.* where they found the level of this proto-oncogene not altered in ALK-positive tumors treated with T20K. Interestingly, when analyzed for another anti-apoptotic member of the BCL-2 family, namely Bcl-xL, the levels were decreased in samples treated with 5μM T20K. A similar effect was stated by Lind *et al*[40]. In conclusion level of anti-apoptotic Bcl-xL was lower what is in agreement with the higher apoptosis depicted by FACS results. It would be interesting to repeat the Western blot analysis with greater number of biological replicates of various AML types to investigate if the observed higher level of Bcl-2 is significant and/or present in different replicates.

We also examined by Western blot the level of ATM. This protein kinase plays a crucial role in inducing cell death during genotoxic stresses. ATM induces apoptosis as a response to DNA

damage. Park *et al*. have recently shown that the ATM/mTOR pathway plays an essential role in the maintenance of protein translation and oxidative phosphorylation, which is critical for cell survival[67]. Other studies implied that targeting the ATM kinase may improve the efficacy of DNA-damaging-based treatment by suppressing DNA repair in cancer cells[68]. The analyzed samples showed similar levels of ATM in the control and 5µM T20K treated samples.

As mentioned earlier, activation of p53 can lead to cell cycle arrest and DNA repair or apoptosis. However, there are also studies suggesting that down-regulation of p53 facilitates apoptosis[51]. In our study, p53 levels were the highest in 5µM T20K treated samples. Higher levels of p53 upon T20K treatment of human lymphoma T-cell lines was also reported by Lind et al.[39] In this study also the role of STAT5 signaling was linked to apoptosis. It would be beneficial to find out if the levels of STAT5 increase after T20K treatment in also in the case of AML cell lines.

Western blot analysis led to interesting preliminary results but for making conclusions we took the levels of samples treated with 5µM into account. Higher levels of T20K drastically lowered the cell viability and one can assume that most of the cells were already dead after 48h, the timepoint of harvesting for the Western blot analysis. This points out again that the 10µM concentration used in the analysis was too high. It seems to be beneficial to repeat the experiments using both, murine and human cell lines, but lower concentrations (i.e., 2,5µM an d 5µM). Moreover, the samples could be harvested for the analysis after 24 and 48h of incubation.

Both tested cyclotides induced apoptosis in the tested murine AML cell lines. That gives the hope for further exploration of this plant derived molecules. They might be useful in AML treatment also in combination with chemotherapy similarly to the small molecule alkaloid emetine. Emetine, commonly used to treat protozoa infections, has been discovered to have immense potential in combating AML. The research has revealed that emetine can specifically target and reduce the viability and clonogenic capacity of AML cells without causing any harm to healthy blood cells. The possibility of emetine working in conjunction with other chemotherapy drugs, such as ara-C, offers a very promising prospect for combinational treatment[69].

6 CONCLUSIONS

We assessed two types of cyclotides: T20K and Caripe. *Möbius* cyclotides strongly interact with membrane components, whereas the bracelet subclass does not. T20K belongs to the *Möbius* subclass and has a cis-Pro residue in loop 5. Meanwhile, Caripe cyclotides belong to the bracelet subclass and have a hydrophobic patch in loop 2[36]. These differences may explain why Caripe and T20K seem to have different mechanisms of action. Both can induce apoptosis, but T20K can also induce necrosis. Further research is needed to shed more light on the mechanisms of these processes.

Cyclotides are a promising source of anti-proliferative substances with immense therapeutic value, owing to their ability to stimulate programmed cell death. Cyclotides have the potential to kill cancer cells by disrupting their membrane properties, which differ from those of healthy cells. This selectivity may be due to the higher concentration of negatively charged phospholipids found in cancer cells[51]. However, the mechanisms by which cyclotides target cancer cells are not fully understood yet. It is crucial to conduct further research to shed light on these mechanisms and potentially pave the way for new cancer treatments.

7 LITERATURE

1. Yamashita M, Iwama A. Aging and Clonal Behavior of Hematopoietic Stem Cells. *Int J Mol Sci*. 2022;23(4):1948. doi:10.3390/ijms23041948

2. Khabusheva E, Spirin P, Lebedev T, Prassolov V. The Role of TAL1 in Hematopoiesis and Leukemogenesis. *Acta Naturae*. 2018;10:15-23.

3. Lai AY, Kondo M. Asymmetrical lymphoid and myeloid lineage commitment in multipotent hematopoietic progenitors. *J Exp Med*. 2006;203(8):1867-1873. doi:10.1084/jem.20060697

4. Pronk CJH, Rossi DJ, Månsson R, et al. Elucidation of the Phenotypic, Functional, and Molecular Topography of a Myeloerythroid Progenitor Cell Hierarchy. *Cell Stem Cell*. 2007;1(4):428-442. doi:10.1016/j.stem.2007.07.005

5. Seita J, Weissman IL. Hematopoietic Stem Cell: Self-renewal versus Differentiation. *Wiley Interdiscip Rev Syst Biol Med*. 2010;2(6):640-653. doi:10.1002/wsbm.86

6. Long NA, Golla U, Sharma A, Claxton DF. Acute Myeloid Leukemia Stem Cells: Origin, Characteristics, and Clinical Implications. *Stem Cell Rev Rep*. 2022;18(4):1211-1226. doi:10.1007/s12015-021-10308-6

7. Wang J, Tomlinson B, Lazarus HM. Update on Small Molecule Targeted Therapies for Acute Myeloid Leukemia. *Curr Treat Options Oncol*. 2023;24(7):770-801. doi:10.1007/s11864-023-01090-3

8. Naeim F, Rao PN. Chapter 11 - Acute Myeloid Leukemia. In: Naeim F, Rao PN, Grody WW, eds. *Hematopathology*. Academic Press; 2008:207-255. doi:10.1016/B978-0-12-370607-2.00011-9

9. Deschler B, Lübbert M. Acute myeloid leukemia: Epidemiology and etiology. *Cancer*. 2006;107(9):2099-2107. doi:10.1002/cncr.22233

10. Crane MM, Strom SS, Halabi S, et al. Correlation between selected environmental exposures and karyotype in acute myelocytic leukemia. *Cancer Epidemiol Biomark Prev Publ Am Assoc Cancer Res Cosponsored Am Soc Prev Oncol*. 1996;5(8):639-644.

11. Acute Myeloid Leukemia - Cancer Stat Facts. SEER. Accessed June 24, 2023. https://seer.cancer.gov/statfacts/html/amyl.html

12. Ohgami RS, Arber DA. The diagnostic and clinical impact of genetics and epigenetics in acute myeloid leukemia. *Int J Lab Hematol*. 2015;37(S1):122-132. doi:10.1111/ijlh.12367

13. Chen KTJ, Gilabert-Oriol R, Bally MB, Leung AWY. Recent Treatment Advances and the Role of Nanotechnology, Combination Products, and Immunotherapy in Changing the Therapeutic Landscape of Acute Myeloid Leukemia. *Pharm Res*. 2019;36(9):125. doi:10.1007/s11095-019-2654-z

14. says SB. Acute Myeloid Leukemia Classification. News-Medical.net. Published November 18, 2010. Accessed July 12, 2023. https://www.news-medical.net/health/Acute-Myeloid-Leukemia-Classification.aspx

15. Hwang SM. Classification of acute myeloid leukemia. *Blood Res*. 2020;55(Suppl):S1-S4. doi:10.5045/br.2020.S001

16. ANGELESCU S, BERBEC NM, COLITA A, BARBU D, LUPU AR. Value of Multifaced Approach Diagnosis and Classification of Acute Leukemias. *Mædica*. 2012;7(3):254-260.

17. What's new in AML Classification (WHO 2022 vs International Consensus…. College of American Pathologists. Accessed July 12, 2023. https://www.cap.org/member-resources/articles/whats-new-in-aml-classification-who-2022-vs-international-consensus-classification

18. Lim SH, Dubielecka PM, Raghunathan VM. Molecular targeting in acute myeloid leukemia. *J Transl Med*. 2017;15(1):183. doi:10.1186/s12967-017-1281-x

19. El-Cheikh J, Bidaoui G, Saleh M, Moukalled N, Abou Dalle I, Bazarbachi A. Venetoclax: A New Partner in the Novel Treatment Era for Acute Myeloid Leukemia and Myelodysplastic Syndrome. *Clin Hematol Int*. 2023;5(2):143-154. doi:10.1007/s44228-023-00041-x

20. Fernandez S, Desplat V, Villacreces A, et al. Targeting Tyrosine Kinases in Acute Myeloid Leukemia: Why, Who and How? *Int J Mol Sci*. 2019;20(14):3429. doi:10.3390/ijms20143429

21. Amanollahi Kamaneh E, Shams Asenjan K, Movassaghpour Akbari A, et al. Characterization of Common Chromosomal Translocations and Their Frequencies in Acute Myeloid Leukemia Patients of Northwest Iran. *Cell J Yakhteh*. 2016;18(1):37-45.

22. Abdel-Wahab O, Levine RL. Mutations in epigenetic modifiers in the pathogenesis and therapy of acute myeloid leukemia. *Blood*. 2013;121(18):3563-3572. doi:10.1182/blood-2013-01-451781

23. Kiyoi H, Kawashima N, Ishikawa Y. FLT3 mutations in acute myeloid leukemia: Therapeutic paradigm beyond inhibitor development. *Cancer Sci*. 2020;111(2):312-322. doi:10.1111/cas.14274

24. Kihara R, Nagata Y, Kiyoi H, et al. Comprehensive analysis of genetic alterations and their prognostic impacts in adult acute myeloid leukemia patients. *Leukemia*. 2014;28(8):1586-1595. doi:10.1038/leu.2014.55

25. Hatlen MA, Wang L, Nimer SD. AML1-ETO driven acute leukemia: insights into pathogenesis and potential therapeutic approaches. *Front Med*. 2012;6(3):248-262. doi:10.1007/s11684-012-0206-6

26. Castiglioni S, Di Fede E, Bernardelli C, et al. KMT2A: Umbrella Gene for Multiple Diseases. *Genes*. 2022;13(3):514. doi:10.3390/genes13030514

27. Górecki M, Kozioł I, Kopystecka A, Budzyńska J, Zawitkowska J, Lejman M. Updates in KMT2A Gene Rearrangement in Pediatric Acute Lymphoblastic Leukemia. *Biomedicines*. 2023;11(3):821. doi:10.3390/biomedicines11030821

28. Craik DJ, Fairlie DP, Liras S, Price D. The Future of Peptide-based Drugs. *Chem Biol Drug Des*. 2013;81(1):136-147. doi:10.1111/cbdd.12055

29. Colgrave ML, Craik DJ. Thermal, Chemical, and Enzymatic Stability of the Cyclotide Kalata B1: The Importance of the Cyclic Cystine Knot. *Biochemistry*. 2004;43(20):5965-5975. doi:10.1021/bi049711q

30. Gran L. Oxytocic principles of Oldenlandia affinis. *Lloydia*. 1973;36(2):174-178.

31. Kremsmayr T, Aljnabi A, Blanco-Canosa JB, Tran HNT, Emidio NB, Muttenthaler M. On the Utility of Chemical Strategies to Improve Peptide Gut Stability. *J Med Chem*. 2022;65(8):6191-6206. doi:10.1021/acs.jmedchem.2c00094

32. Gupta R, Kumari J, Pati S, Singh S, Mishra M, Ghosh SK. Interaction of cyclotide Kalata B1 protein with model cellular membranes of varied electrostatics. *Int J Biol Macromol*. 2021;191:852-860. doi:10.1016/j.ijbiomac.2021.09.147

33. Göransson U, Craik DJ. Disulfide Mapping of the Cyclotide Kalata B1. *J Biol Chem*. 2003;278(48):48188-48196. doi:10.1074/jbc.M308771200

34. Herrmann A, Burman R, Mylne JS, et al. The alpine violet, Viola biflora, is a rich source of cyclotides with potent cytotoxicity. *Phytochemistry*. 2008;69(4):939-952. doi:10.1016/j.phytochem.2007.10.023

35. Camarero JA. Cyclotides, a versatile ultrastable micro-protein scaffold for biotechnological applications. *Bioorg Med Chem Lett*. 2017;27(23):5089-5099. doi:10.1016/j.bmcl.2017.10.051

36. Falanga CM, Steinborn C, Muratspahić E, et al. Ipecac root extracts and isolated circular peptides differentially suppress inflammatory immune response characterised by

proliferation, activation and degranulation capacity of human lymphocytes in vitro. *Biomed Pharmacother*. 2022;152:113120. doi:10.1016/j.biopha.2022.113120

37. Gründemann C, Stenberg KG, Gruber CW. T20K: An Immunomodulatory Cyclotide on Its Way to the Clinic. *Int J Pept Res Ther*. 2019;25(1):9-13. doi:10.1007/s10989-018-9701-1

38. Thell K, Hellinger R, Sahin E, et al. Oral activity of a nature-derived cyclic peptide for the treatment of multiple sclerosis. *Proc Natl Acad Sci*. 2016;113(15):3960-3965. doi:10.1073/pnas.1519960113

39. Lind J, Hellinger R, Kudweis P, et al. The nature inspired peptide [T20K]-kalata B1 induces anti-tumor effects in anaplastic large cell lymphoma. *Biomed Pharmacother*. 2022;153:113486. doi:10.1016/j.biopha.2022.113486

40. Lind J, Hellinger R, Kudweis P, et al. The nature inspired peptide [T20K]-kalata B1 induces anti-tumor effects in anaplastic large cell lymphoma. *Biomed Pharmacother*. 2022;153:113486. doi:10.1016/j.biopha.2022.113486

41. Gründemann C, Thell K, Lengen K, et al. Cyclotides Suppress Human T-Lymphocyte Proliferation by an Interleukin 2-Dependent Mechanism. *PLOS ONE*. 2013;8(6):e68016. doi:10.1371/journal.pone.0068016

42. Jackson MA, Xie J, Nguyen LTT, et al. Plant-based production of an orally active cyclotide for the treatment of multiple sclerosis. *Transgenic Res*. 2023;32(1):121-133. doi:10.1007/s11248-023-00341-1

43. Lee MR. Ipecacuanha: the South American vomiting root. *J R Coll Physicians Edinb*. 2008;38(4):355-360.

44. Fahradpour M, Keov P, Tognola C, et al. Cyclotides Isolated from an Ipecac Root Extract Antagonize the Corticotropin Releasing Factor Type 1 Receptor. *Front Pharmacol*. 2017;8:616. doi:10.3389/fphar.2017.00616

45. Taghizadeh MS, Retzl B, Muratspahić E, et al. Discovery of the cyclotide caripe 11 as a ligand of the cholecystokinin-2 receptor. *Sci Rep*. 2022;12(1):9215. doi:10.1038/s41598-022-13142-z

46. Fahradpour M, Keov P, Tognola C, et al. Cyclotides Isolated from an Ipecac Root Extract Antagonize the Corticotropin Releasing Factor Type 1 Receptor. *Front Pharmacol*. 2017;8. Accessed August 1, 2023. https://www.frontiersin.org/articles/10.3389/fphar.2017.00616

47. Doma E, Mayer IM, Brandstoetter T, et al. A robust approach for the generation of functional hematopoietic progenitor cell lines to model leukemic transformation. *Blood Adv*. 2020;5(1):39-53. doi:10.1182/bloodadvances.2020003022

48. Schmalzbauer BS, Thondanpallil T, Heller G, et al. CDK6 Degradation Is Counteracted by p16INK4A and p18INK4C in AML. *Cancers*. 2022;14(6):1554. doi:10.3390/cancers14061554

49. Berrouet C, Dorilas N, Rejniak KA, Tuncer N. Comparison of Drug Inhibitory Effects (IC50) in Monolayer and Spheroid Cultures. *Bull Math Biol*. 2020;82(6):68. doi:10.1007/s11538-020-00746-7

50. Esmaeili MA, Abagheri-Mahabadi N, Hashempour H, Farhadpour M, Gruber CW, Ghassempour A. Viola plant cyclotide vigno 5 induces mitochondria-mediated apoptosis via cytochrome C release and caspases activation in cervical cancer cells. *Fitoterapia*. 2016;109:162-168. doi:10.1016/j.fitote.2015.12.021

51. Mehta L, Dhankhar R, Gulati P, Kapoor RK, Mohanty A, Kumar S. Natural and grafted cyclotides in cancer therapy: An insight. *J Pept Sci*. 2020;26(4-5):e3246. doi:10.1002/psc.3246

52. Xu S, Li X, Zhang J, Chen J. Prognostic Value of CD11b Expression Level for Acute Myeloid Leukemia Patients: A Meta-Analysis. *PLoS ONE*. 2015;10(8):e0135981. doi:10.1371/journal.pone.0135981

53. Bradfute SB, Graubert TA, Goodell MA. Roles of Sca-1 in hematopoietic stem/progenitor cell function. *Exp Hematol*. 2005;33(7):836-843. doi:10.1016/j.exphem.2005.04.001

54. Hu Q, Peng J, Liu W, et al. Elevated cleaved caspase-3 is associated with shortened overall survival in several cancer types. *Int J Clin Exp Pathol*. 2014;7(8):5057-5070.

55. Ježek J, Smethurst DGJ, Stieg DC, et al. Cyclin C: The Story of a Non-Cycling Cyclin. *Biology*. 2019;8(1):3. doi:10.3390/biology8010003

56. Kawabata KC, Zong H, Meydan C, et al. BCL6 maintains survival and self-renewal of primary human acute myeloid leukemia cells. *Blood*. 2021;137(6):812-825. doi:10.1182/blood.2019001745

57. Fernando TM, Marullo R, Gresely BP, et al. BCL6 evolved to enable stress tolerance in vertebrates and is broadly required by cancer cells to adapt to stress. *Cancer Discov*. 2019;9(5):662-679. doi:10.1158/2159-8290.CD-17-1444

58. Minn AJ, Kettlun CS, Liang H, et al. Bcl-xL regulates apoptosis by heterodimerization-dependent and -independent mechanisms. *EMBO J*. 1999;18(3):632-643. doi:10.1093/emboj/18.3.632

59. Shiloh Y, Ziv Y. The ATM protein kinase: regulating the cellular response to genotoxic stress, and more. *Nat Rev Mol Cell Biol*. 2013;14(4):197-210. doi:10.1038/nrm3546

60. Levine AJ. p53, the Cellular Gatekeeper for Growth and Division. *Cell*. 1997;88(3):323-331. doi:10.1016/S0092-8674(00)81871-1

61. Hughes PJ, Marcinkowska E, Gocek E, Studzinski GP, Brown G. Vitamin D3-driven signals for myeloid cell differentiation—Implications for differentiation therapy. *Leuk Res*. 2010;34(5):553-565. doi:10.1016/j.leukres.2009.09.010

62. Gocek E, Marcinkowska E. Differentiation Therapy of Acute Myeloid Leukemia. *Cancers*. 2011;3(2):2402-2420. doi:10.3390/cancers3022402

63. Li N, Fassl A, Chick J, et al. Cyclin C is a haploinsufficient tumor suppressor. *Nat Cell Biol*. 2014;16(11):1080-1091. doi:10.1038/ncb3046

64. Wang K, Yan R, Cooper KF, Strich R. Cyclin C mediates stress-induced mitochondrial fission and apoptosis. *Mol Biol Cell*. 2015;26(6):1030-1043. doi:10.1091/mbc.E14-08-1315

65. Barczyk K, Kreuter M, Pryjma J, et al. Serum cytochrome c indicates in vivo apoptosis and can serve as a prognostic marker during cancer therapy. *Int J Cancer*. 2005;116(2):167-173. doi:10.1002/ijc.21037

66. Hafezi S, Rahmani M. Targeting BCL-2 in Cancer: Advances, Challenges, and Perspectives. *Cancers*. 2021;13(6):1292. doi:10.3390/cancers13061292

67. Park HJ, Gregory MA, Zaberezhnyy V, et al. Therapeutic resistance in acute myeloid leukemia cells is mediated by a novel ATM/mTOR pathway regulating oxidative phosphorylation. Henske EP, Rathmell WK, eds. *eLife*. 2022;11:e79940. doi:10.7554/eLife.79940

68. Wang YC, Lee KW, Tsai YS, et al. Downregulation of ATM and BRCA1 Predicts Poor Outcome in Head and Neck Cancer: Implications for ATM-Targeted Therapy. *J Pers Med*. 2021;11(5):389. doi:10.3390/jpm11050389

69. Cornet-Masana JM, Moreno-Martínez D, Lara-Castillo MC, et al. Emetine induces chemosensitivity and reduces clonogenicity of acute myeloid leukemia cells. *Oncotarget*. 2016;7(17):23239-23250. doi:10.18632/oncotarget.8096

ACKNOWLEDGMENTS

Above all else, I want to express my deep gratitude to Karoline Kollmann for providing me with the incredible opportunity to work in the laboratory. Karoline also acted as my supervisor, guiding me through the entire process from planning my experiments to discussing the results and helping me write my thesis. She was always available to offer advice and support, and I couldn't have done it without her.

I must also acknowledge Belinda Schmalzbauer, who has been my biggest support over the past nine months. She taught me to think scientifically and patiently introduced me to new laboratory methods. Belinda's positivity and enthusiasm for the field of research made her an outstanding mentor, and I'll always cherish the memories of our time together.

I also want to thank my husband for his unwavering support throughout this process. I wouldn't be at this point without him.

Finally, I can't forget all of the other laboratory members, family, and friends who helped make this journey possible for me. Their encouragement and motivation were invaluable to me during my master's thesis.